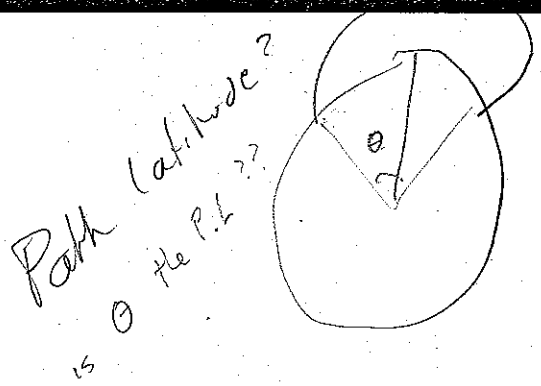

# VERY LOW FREQUENCY RADIO WAVES IN THE MAGNETOSPHERE

C. G. PARK AND D. L. CARPENTER

*Radioscience Laboratory, Stanford University, Stanford, California 94305*

CONTENTS



## 1. INTRODUCTION

The topic of this chapter is very low frequency, or VLF (~100 Hz to ~100 kHz), wave phenomena and their applications as diagnostic tools in magnetospheric research. These waves propagate through the magnetosphere in what is known as the 'whistler mode,' a reference to the fact that this mode explains the propagation of lightning-induced whistlers. Some authors refer to all electromagnetic waves propagating in this mode as whistlers, but here we will avoid confusion by reserving that term for waves originating in lightning discharges. Whistler mode propagation is possible only in the presence of a magnetic field and at frequencies below the electron gyrofrequency, the natural frequency of cyclotron motion of electrons about the direction of the magnetic field. By contrast, high-frequency propagation is possible only above the plasma frequency, a natural oscillation frequency of the plasma. Under ordinary circumstances the plasma frequency is much higher than the electron gyrofrequency throughout the plasmasphere or inner magnetosphere and near the magnetic equator in the more distant regions. The geomagnetic field thus provides a low-frequency passband within which a wide variety of wave and wave-particle interaction phenomena may take place.

Whistler mode waves propagate at velocities well below the propagation speed in a vacuum. The group velocities are strongly dependent on frequency, so that distinctive, readily identified wave forms are received. Furthermore, the slow phase velocities allow the waves to interact strongly with energetic electrons, a phenomenon resulting in wave growth and particle precipitation.

In the whistler mode, wave normal direction and ray path are strongly affected by the geomagnetic field as well as by density gradients. The geomagnetic field tends to guide rays in the field line direction, but magnetic guiding alone is not sufficient to make them follow the curving field lines exactly. Figure 1.1*a* illustrates a ray path in a magnetosphere in which plasma densities decrease smoothly with distance. The wave frequency is ~1 kHz; waves propagating in this 'unducted mode' may undergo a number of reversals of direction in regions where the local lower hybrid resonance (LHR) frequency of the plasma is equal to the wave frequency [*Edgar*, 1972, 1976]. Their propagation gives rise to many interesting phenomena that can be observed by satellites. However, these subjects are beyond the scope of this chapter.

While unducted whistler mode propagation de-

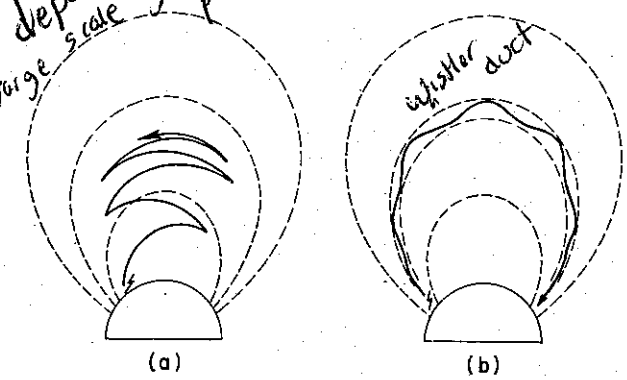


Fig. 1.1. Typical whistler ray path in (*a*) unducted mode and (*b*) ducted mode. Dashed lines represent geomagnetic field lines.

pends strongly on the large-scale gradients of plasma density, ground-observed events depend upon the presence in the magnetosphere of density irregularities of varying sizes. Electron density gradients associated with field-aligned irregularities can trap whistler mode waves and guide them in such a way that both the wave normal angle and the ray-path direction are confined within a small cone about the field lines [*Smith*, 1961*a*; *Helliwell*, 1965]. Figure 1.1*b* illustrates schematically a snakelike ray path inside such a 'whistler duct.' If the ducting effect continues down to ionospheric heights in the conjugate ionosphere, the ducted waves can penetrate the ionosphere and, after propagating in the earth-ionosphere wave guide, be observed at ground stations within a radius of ~1000 km of the exit point.

A typical duct may measure a few hundred kilometers in diameter at the equator and have density enhancements of the order of 10% or more above the background level [*Angerami*, 1970]. There may be as many as 30 or more ducts within the viewing range of a whistler receiver, part or all of which may be illuminated by a given lightning discharge. This allows simultaneous probing of a large volume in the magnetosphere ($2 \leq L \leq 6$, ~±20° longitude) from a single ground station. Furthermore, because of the long-enduring nature of whistler ducts it is possible to monitor the same plasma continuously for many hours. These factors make whistlers a powerful diagnostic tool.

Historically, whistlers provided the first evidence that the earth's plasma envelope extended far beyond the normal ionospheric *F* layer heights [*Storey*, 1953]. This opened a vast new region for exploration which later came to be called the protonosphere or magnetosphere. The discovery of nose whistlers [*Helliwell et al.*, 1956] a few years later made it possible to determine the magnetic shell coordinate of a whistler path (equatorial radius or endpoint latitude) and permitted more detailed studies of plasma distribution in the magnetosphere [*Smith*, 1960, 1961*b*]. This in turn led to the discovery of the plasmapause [*Carpenter*, 1962, 1963, 1966], a field-aligned boundary at which the equatorial electron concentration may drop abruptly from a few hundred per cubic centimeter to a few per cubic centimeter within a fraction of an earth radius. The dense region inside the plasmapause is called the plasmasphere.

An extensive survey of whistler and other VLF wave activity was conducted during and immediately following the International Geophysical Year (IGY), 1957–1958, with some 50 monitoring stations extending from the equator to the poles. It soon became clear that Antarctica was an ideal place for VLF research, and substantial VLF research efforts were launched at a few key antarctic stations. The favorable factors in Antarctica include low levels of both man-made and natural electromagnetic noise such as sferics, low ionospheric absorption during long winter nights, and exceptionally high whistler rates. The Eights-Siple area in Antarctica has the world's highest whistler rates, often exceeding one whistler per second during austral winter. This is due to the fact that the conjugate region in northeastern North America provides excellent lightning sources at relatively high geomagnetic latitudes. Whistlers recorded at Eights (1963–1965) led to a number of important breakthroughs; this provided a strong motivation to establish Siple Station in the same general area. Winter-over operations at Siple started in 1973.

It is convenient to divide the discussion of VLF phenomena into two parts. In the first part we discuss the dynamics of the thermal plasma (energies of <~10 eV) in the magnetosphere, deduced from the dispersion characteristics of whistlers. The second part deals with the effects of energetic electrons (energies of >~100 eV) that give the magnetosphere its amplifier-oscillator properties. Energetic electrons are not usually present in sufficient numbers to affect the propagation characteristics of the waves but have sufficient energy fluxes to cause strong wave growth.

## 2. WHISTLER STUDIES OF PLASMASPHERE DYNAMICS

Whistler probing of the structure and dynamics of the magnetospheric thermal plasma is important for many reasons. This plasma provides a reservoir for the underlying ionosphere. It also forms the dense

'cool' background that is threaded by the radiation belts, which represent the much more tenuous but far more energetic component of the plasma. The cool and hot magnetospheric plasmas interact in important but subtle ways. For example, the thermal plasma controls the wave refractive index and thus determines certain conditions of interaction between VLF waves and high-energy particles.

Through measurements of the topology of the plasmapause and of the cross-$L$ motions of whistler paths the whistler technique provides information on magnetospheric convection, the circulation induced by the 'wind' of solar plasma in its encounter with the earth's magnetosphere. The whistler technique also provides important information on the complex magnetospheric substorm, a disturbance event of fundamental importance in which stored energy is dramatically redistributed and dissipated.

### 2.1. *Whistler Technique*

The success of whistler diagnostics of the plasmasphere derives from the excellent agreement between observed whistler frequency versus time characteristics and the predictions of a relatively straightforward propagation theory. For longitudinal propagation in a ducted mode the whistler travel time can be closely approximated by [*Helliwell*, 1965]

$$t(f) = \int \frac{ds}{v_g} = \frac{1}{2cf^{1/2}} \int \frac{f_p}{f_H^{1/2}[1-(f/f_H)]^{3/2}}\, ds \qquad (2.1)$$

where $v_g$ is the group velocity, $ds$ is an element of length along a field-aligned path, $c$ is the speed of light in free space, $f$ is the wave frequency, $f_H$ is the electron gyrofrequency, and $f_p$ is the plasma frequency. The integration is over the entire path above the lower edges of the ionosphere. If we adopt any reasonable field line distribution models for $f_H$ and $f_p$, the resulting $t(f)$ curve accurately describes the shape of whistlers as illustrated in Figure 2.1. The frequency of minimum travel time is called the nose frequency $f_n$; it is roughly proportional to the minimum electron gyrofrequency along the path ($f_{Heq}$). The 'constant' of proportionality is weakly dependent on the path latitude as well as on the field line distribution models of $f_p$ and $f_H$. For a diffusive equilibrium model, $f_n \simeq 0.37 f_{Heq}$, while for a collisionless model that might apply when plasma densities are extremely low we obtain $f_n \simeq 0.41 f_{Heq}$. Once $f_{Heq}$ is known, it is straightforward to determine the path equatorial radius from the $f_H$ model. If a part of a whistler containing the nose is not visible on a spectrogram, it can be reconstructed from visible portions of the whistler trace by using one of several curve-fitting techniques that have been developed recently (see, for example, *Ho and Bernard* [1973], *Smith et al.* [1974], *Corcuff and Corcuff* [1973], and *Tarcsai* [1975]).

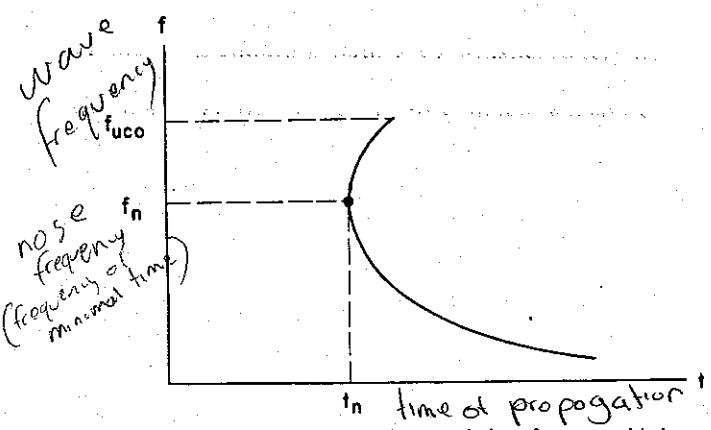


Fig. 2.1. Frequency-time characteristics of a nose whistler.

A measurement of $t_n$ for a given path provides a scale factor for the assumed field line model of the distribution of $f_p$. Since plasma frequency $f_p$ is proportional to $n_e^{1/2}$, where $n_e$ is the electron density, an estimate of electron densities everywhere along the path can thus be made. For reasons discussed below, electron density estimates near the equator are much less model dependent than those at low altitudes. A very useful parameter, which is even less model dependent than equatorial density, is tube content $N_T$. It is commonly defined as the total number of electrons in a flux tube extending from 1000-km altitude to the equator and having 1-cm$^2$ cross-sectional area at the base.

An abrupt upper cutoff frequency of whistlers, $f_{uco}$, is believed to be determined by trapping conditions inside enhancement ducts. Propagation theory predicts that trapping should be effective only at frequencies below $f_H/2$ [*Smith*, 1961*a*]; hence waves whose frequencies exceed $f_{Heq}/2$ should leak out of ducts before they reach the equator and fall into the unducted regime. This has been verified by satellite observations of leakage from ducts [*Angerami*, 1970] as well as by statistical studies of ground whistlers [*Carpenter*, 1968].

Figure 2.2 shows two examples of whistlers along with equatorial electron density profiles deduced from them. In each spectrogram the causative sferic is marked by an arrow. The smooth $f_n$-$t_n$ locus in the first whistler yields a correspondingly smooth electron density profile as indicated by solid circles.

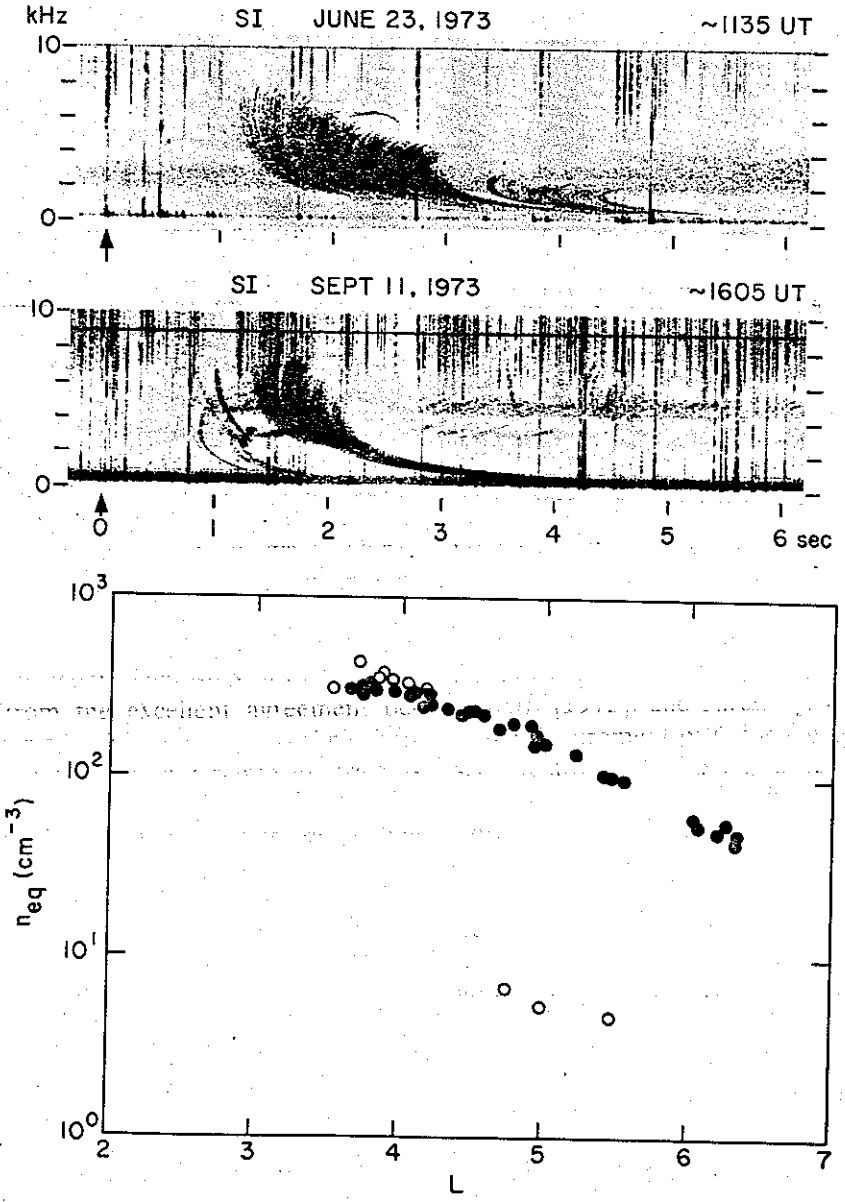


Fig. 2.2. Frequency-time spectrograms of two whistlers recorded at Siple, Antarctica. Arrows mark the causative sferics. The lower plot shows equatorial electron density profiles deduced from the two whistlers: solid circles, June 23 whistler; open circles, September 11 whistler.

In the case of the second whistler the $f_n$-$t_n$ locus is irregular. At low values of $f_n$, nose travel time $t_n$ is also low; this is due to the density drop at the plasmapause, located in this case near $L = 4.5$ (open circles). In the analysis the geomagnetic field was approximated by a centered dipole. A diffusive equilibrium model of plasma density was used inside the plasmapause, and a collisionless model was used outside. Evidence in support of this choice of models was found by *Angerami* [1966] and *Angerami and Carpenter* [1966]. However, since collisions must occur at some finite rate, collisionless models represent idealized situations that may be approached only if electron densities are extremely low. In most cases, including the case under discussion here, the use of a collisionless model probably underestimates equatorial densities by factors of up to about 2.

Returning to (2.1), we see that the integral is heavily weighted in favor of the equatorial region, where $f_H$ is small. For $L \geq 2$ it is found that about 80% of the whistler propagation delay occurs within $\pm 30°$ of the equator, where both $f_p$ and $f_H$ vary

slowly with distance along field lines. Thus the equatorial parameters deduced from whistlers are remarkably insensitive to assumed field line distribution of $f_p$ and $f_H$. Inside the plasmapause, typical model-dependent errors in $f_{Heq}$, $n_{eq}$, and $N_T$ are estimated to be less than 1%, 10%, and 4%, respectively. Outside the plasmapause the use of a collisionless model may cause $f_{Heq}$, $n_{eq}$, and $N_T$ to be underestimated by as much as 10%, 50%, and 10%, respectively. A detailed analysis of the whistler technique, including model-dependent and other sources of error, can be found in a study by *Park* [1972].

### 2.2. *The Plasmapause*

The first measurements of the density gradients associated with the plasmapause were made during the IGY by whistler techniques [*Carpenter,* 1963] and by two USSR lunar probes [*Gringauz et al.*, 1960]. The Lunik probes provided in situ evidence of steep gradients in positive ions, while the whistler data indicated that the corresponding knee or density gradient in the electrons was of frequent occurrence and that its equatorial distance varied inversely with magnetic activity. The recognition of the regular existence of a worldwide boundary and its identification as the 'plasmapause' followed further studies based on antarctic whistlers (described below). In the middle and late 1960s, satellite measurements in the pioneering Ogo series helped to confirm and extend the whistler results [*Taylor et al.*, 1965; *Chappell et al.*, 1970]. Although it had not been predicted theoretically, the plasmapause rapidly gained general acceptance. Today it is recognized as an important boundary not only because its dynamic behavior serves as an indicator of large-scale magnetospheric convection activity [e.g., *Axford*, 1969], but also because the sharp density drop across the field-aligned boundary gives rise to a variety of interesting phenomena. Examples include special classes of VLF [e.g., *Carpenter et al.*, 1968] and ULF [e.g., *Lanzerotti et al.*, 1974] phenomena, strong pitch angle diffusion of energetic particles [e.g., *Williams and Lyons*, 1974], and the excitation of stable red auroral arcs [e.g., *Hoch*, 1973].

The plasmapause has also been associated with a number of ionospheric features such as the mid-latitude electron density trough [e.g., *Muldrew,* 1965] and the light ion trough [e.g., *Taylor and Walsh*, 1972]. However, the coupling between the equatorial plasmapause region and the underlying ionosphere is a complex problem; depending on geomagnetic conditions, the two regions may be dominated by fundamentally different physical processes. For example, a stable nighttime ionosphere is expected to reflect the presence of the equatorial plasmapause, but not if the ionosphere is sunlit or is disturbed by some other process [*Park and Banks*, 1975; *Grebowsky et al.*, 1977]. More experimental and theoretical work is needed before ionospheric observations can be used for tracking the plasmapause position. We will now review properties of the plasmapause deduced from whistler observations.

Early whistler data from the northern hemisphere IGY network and from Byrd Station, Antarctica, suggested that the plasmapause, or 'knee' as it was then called, was a persistent feature of the magnetosphere [*Carpenter*, 1963]. There was a need for better experimental evidence on this point. Several-day-long time series of data on plasmapause position were needed in order to identify diurnal effects and responses to changes in magnetic activity. Data of this type became available after broadband VLF recordings were initiated at Eights Station in 1963. Some of the key findings follow.

*Electron density and tube content near the plasmapause.* At the knee, or plasmapause, equatorial electron density decreases with distance by a factor of 30–100, while tube content decreases by a factor of about 10. The equatorial density decrease may take place within $<0.15\ R_E$ and the content change within $<1°$ latitude at 1000 km.

Density and content profiles representing moderately disturbed magnetic conditions were obtained for both the nightside and the dayside of the earth [*Angerami and Carpenter,* 1966]. These results provided some of the first clear evidence of the essentially worldwide nature of the plasmapause.

*Diurnal variation of the plasmapause position.* In July 1963 there were several weak magnetic storms; the plasmapause radius exhibited a generally repeatable and distinctive diurnal pattern during the several days of relatively steady but moderate geomagnetic agitation ($Kp$ = 2–4) that followed the onset of each storm [*Carpenter*, 1966]. Figure 2.3 shows whistler data on plasmapause radius in earth radii versus universal time and magnetic local time at Eights on four successive days, July 7–10, 1963. At the end of each panel are periods of overlap with the preceding and following days. The daily mean values of plasmapause radius are in the range 3.5–4.0 $R_E$. There is a minimum radius in the dawn sector and a maximum in the premidnight sector; the difference between the maximum and minimum radii is about 1.5 $R_E$.

Figure 2.4 shows this behavior on a polar plot of

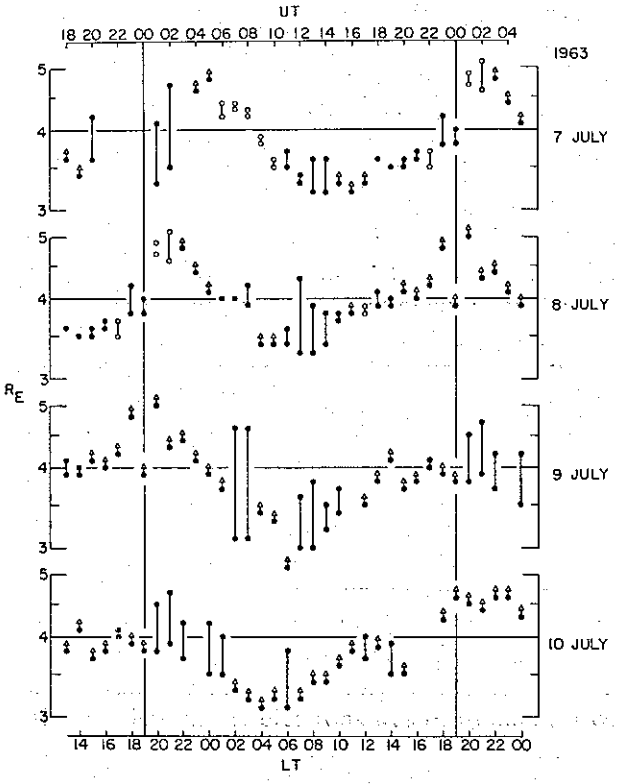


Fig. 2.3. Variation of the plasmapause position in units of earth radii plotted against time for four consecutive days in July 1963. The data for 3 hours before and after 00 UT are repeated in each panel. The observations were made at Eights, Antarctica. Open or solid circles connected by a line represent the range within which the plasmapause lies. An arrow connected to a data point represents an inner limit of the plasmapause position [from *Carpenter*, 1966].

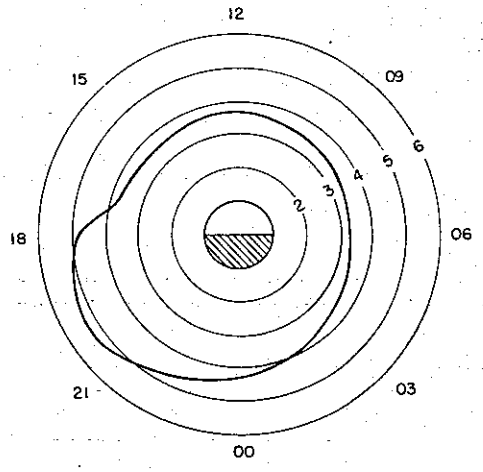


Fig. 2.4. The average equatorial radius of plasmapause versus local time under moderately disturbed magnetic conditions ($Kp$ = 2–4). The observations were made in July and August 1963 at Eights, Antarctica (adapted from *Carpenter* [1966]).

equatorial radius versus magnetic local time. The solid curve represents an average of July–August 1963 days of moderate steady agitation (such as those in Figure 2.3). There is a rapid change in radius with local time near 18 LT associated with the region of larger radius called the 'bulge.' Because of the repeatability and the extent of the data it was inferred that the solid curve of Figure 2.4, a result of averaging over time, represents the large-scale spatial characteristics of the plasmapause under conditions of moderate steady magnetic agitation.

*Response of the plasmapause to magnetic disturbance.* Earlier whistler studies had suggested that the plasmapause radius decreases with increasing magnetic activity [*Carpenter*, 1963]. The data from Eights provided extensive new documentation of this effect. Figures 2.5*a* and 2.5*b* display plasmapause position data during two 4-day periods. The periods had approximately similar magnetic disturbance histories as shown by the $Kp$ index (values increasing downward). Two days of quieting were followed by weak gradual-commencement magnetic storms. The plasmapause response was similar in the two cases. During the two initial days of quieting there was a generally increasing trend in the radius. Then during the first storm day the radius dropped to a minimum of 3.0–3.5 $R_E$. A diurnal pattern similar to the patterns of Figure 2.3 then developed on the fourth day as the several-day recovery phase of the storms began.

Significant inward displacements of the plasmapause, observed from a ground station, were thus found to occur within a period of the order of 6 hours following an increase in the worldwide disturbance index. Later studies showed that in a worldwide sense the disturbance response of the plasmasphere is very complicated, owing in part to the inhomogeneity of the coupled magnetosphere-ionosphere system and to spatial and temporal limits on disturbance activity.

*Physical interpretation of the plasmapause phenomenon.* The relatively low densities beyond the plasmapause are generally attributed to coupling of this outer region to more distant regions of low plasma density such as the magnetotail [e.g., *Nishida*, 1966] or interplanetary space [e.g., *Brice*, 1967]. The coupling is believed to occur through the combined effects of solar wind induced magnetospheric convection and a flow regime associated with the earth's rotation. The combined effects of the two regimes are such that in an inner magnetospheric region the flow lines enclose the earth. The plasmapause represents the outer limit of this region; beyond it the plasma circulates so as to be carried to and from the outer reaches of the magne-

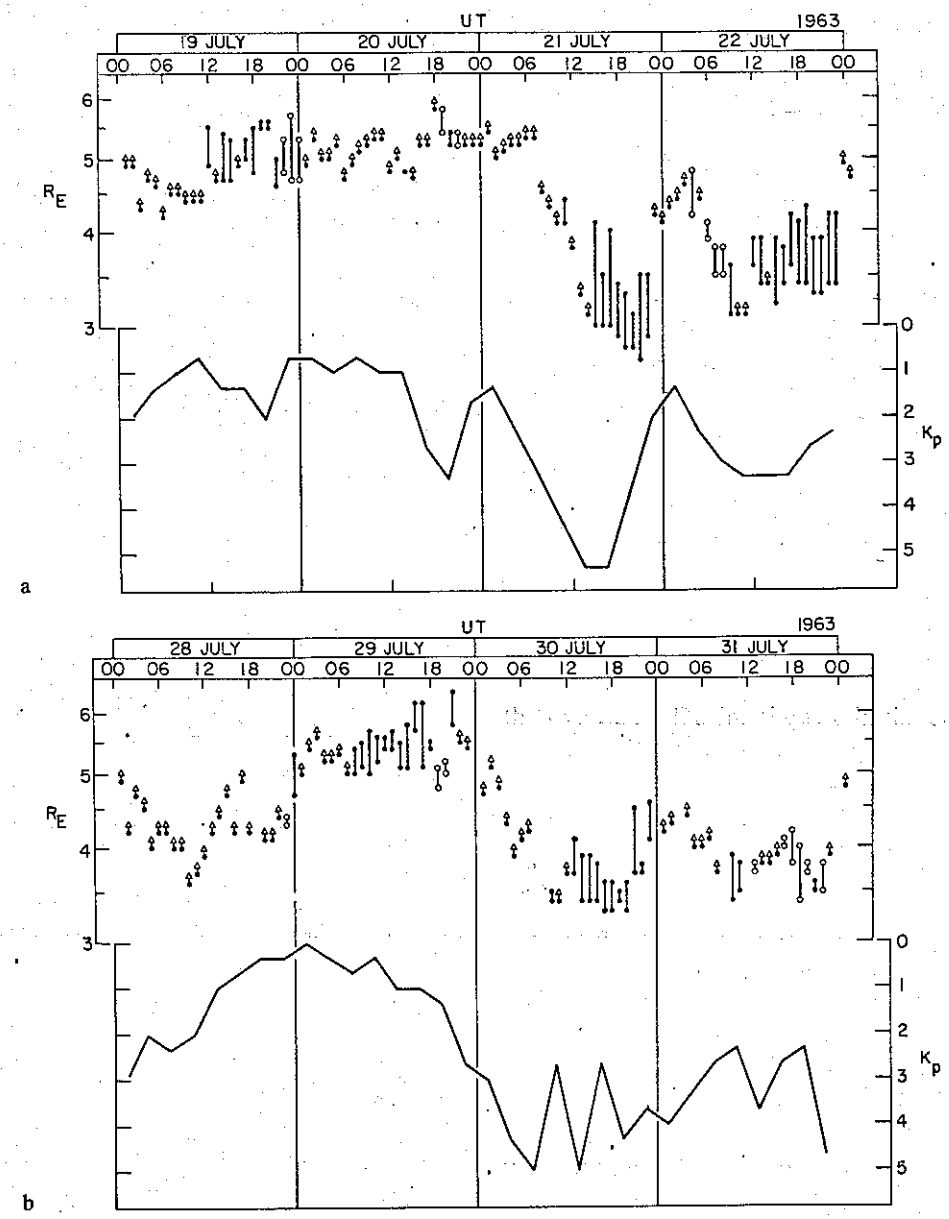


Fig. 2.5. Comparison of the plasmapause equatorial radius observed at Eights, Antarctica, with *Kp* [from *Carpenter*, 1966].

tosphere. When the high-altitude portions of a convecting field-aligned region temporarily reach the magnetotail or interplanetary space, enhanced upflows of plasma can occur, effectively evacuating the region and giving rise to the low average density level observed beyond the plasmapause.

A number of important interpretive ideas were developed by *Brice* [1967], who noted the evening bulge or local time asymmetry in plasmapause radius, and interpreted this effect as being due to local opposition of the flow associated with the earth's rotation by a large-scale sunward flow associated with a dawn-dusk electric field in the magnetosphere. Figure 2.6, reproduced from *Brice*'s [1967] Figure 15, shows postulated equatorial flow patterns.

Although these ideas continue to be widely accepted, continuing research has shown the plasmapause-plasmasphere system to be a complex dynamical phenomenon. Interpretive models capable of reproducing the known complexities are only gradually being developed; the models require information on magnetospheric electric fields and on complex ionization interchange processes along geomagnetic field lines. These are subject areas in which much remains to be done both experimentally and

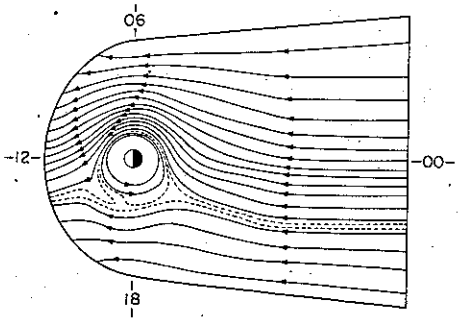


Fig. 2.6. A model of plasma flow pattern in the equatorial magnetosphere (adapted from *Brice* [1967]).

theoretically and in which antarctic researchers have a major continuing interest (see later sections).

*The plasmasphere bulge.* The dynamic nature of the plasmasphere was evidenced in studies of the bulge or duskside increase in plasmapause radius [*Carpenter,* 1970]. It was found that the local time at which a ground station first detects the westward end of the bulge depends on magnetospheric substorm activity. The earlier local times, near dusk and in the afternoon sector, were associated with periods of increasing or sustained substorm activity, while later times, between dusk and midnight, were associated with quieting. These observations of the plasmapause boundary were interpreted as evidence of sunward surges of plasma in the duskside plasmasphere during substorms, coupled with a tendency for the outer plasmasphere to move in the direction of the earth's rotation during quieting. In these studies it was inferred that the dusk sector is a region of exceptionally intense plasma flow activity in the middle magnetosphere. Related findings from spacecraft and from ground-based probing techniques at high latitudes have confirmed and extended this picture. Ogo 5 satellite data on outlying plasma structures or 'detached plasmas' at 6–9 $R_E$ suggest that such structures develop in the dusk sector during substorm flow activity [*Chappell,* 1974]. High-latitude measurements of plasma flow or associated electric fields at ionospheric heights show relatively large sunward flow activity in the dusk and dawn sectors [*Cauffman and Gurnett,* 1972; *Heppner,* 1972; *Mozer,* 1976; *Banks et al.,* 1973].

*Propagation effects at the plasmapause.* The plasmapause appears to serve as a guide and a trap of VLF waves in a manner that is not yet well understood. In most cases of plasmasphere propagation and frequently in ducted propagation well beyond the plasmapause, there is an intensity cutoff in whistlers at about $1.3f_n$, which corresponds (from dispersion analysis) to $f_{Heq}/2$, or half the equatorial gyrofrequency of the path [*Carpenter,* 1968]. However, whistlers propagating just outside the boundary frequently extend well above this limit. Figure 2.7 shows two examples recorded 1 hour apart on June 9, 1965, at Eights, Antarctica. Both events extend to $\simeq 2f_n$, or to $\simeq 0.8f_{Heq}$.

Propagation just beyond the plasmapause may include multihop echoing above $f_{Heq}/2$, an effect not observed in ordinary ducted propagation. On some occasions the activity includes noise bands near or above $f_{Heq}/2$. Figure 2.8 shows an example of such activity following the development of a moderate magnetic storm on July 6, 1965. The upper part of the figure shows 1-min samples of VLF spectra recorded at Eights, Antarctica, at 15-min intervals over a roughly 3-hour period from 1450 to 1736 UT. Below the broadband records is part of a continuous chart recording of wave field strength in microvolts per meter in the band 7–12 kHz. Data from 1400 to 1600 UT are shown. The five times at which synoptic recordings are available on the panels above are noted by arrows above the chart. The corresponding spectra are marked by asterisks.

Banded noise activity is present during most of the approximately 3-hour period represented by the VLF spectra. The frequency, the intensity, and the bandwidth of the bands vary with time; occasionally, there are two bands. On the 1720 UT record a new band develops as an existing one continues. Near 1520 and 1535 UT there appear to be quasi-periodic increases in band center frequency with time; the oscillations on the chart below suggest that new

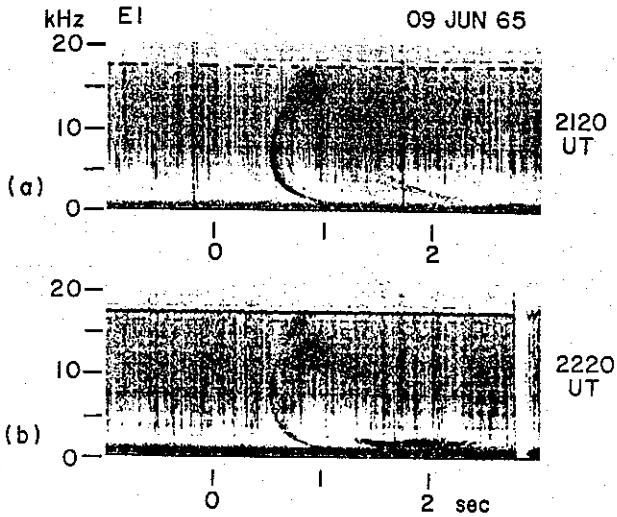


Fig. 2.7. Two examples of whistlers propagating just outside the plasmapause.

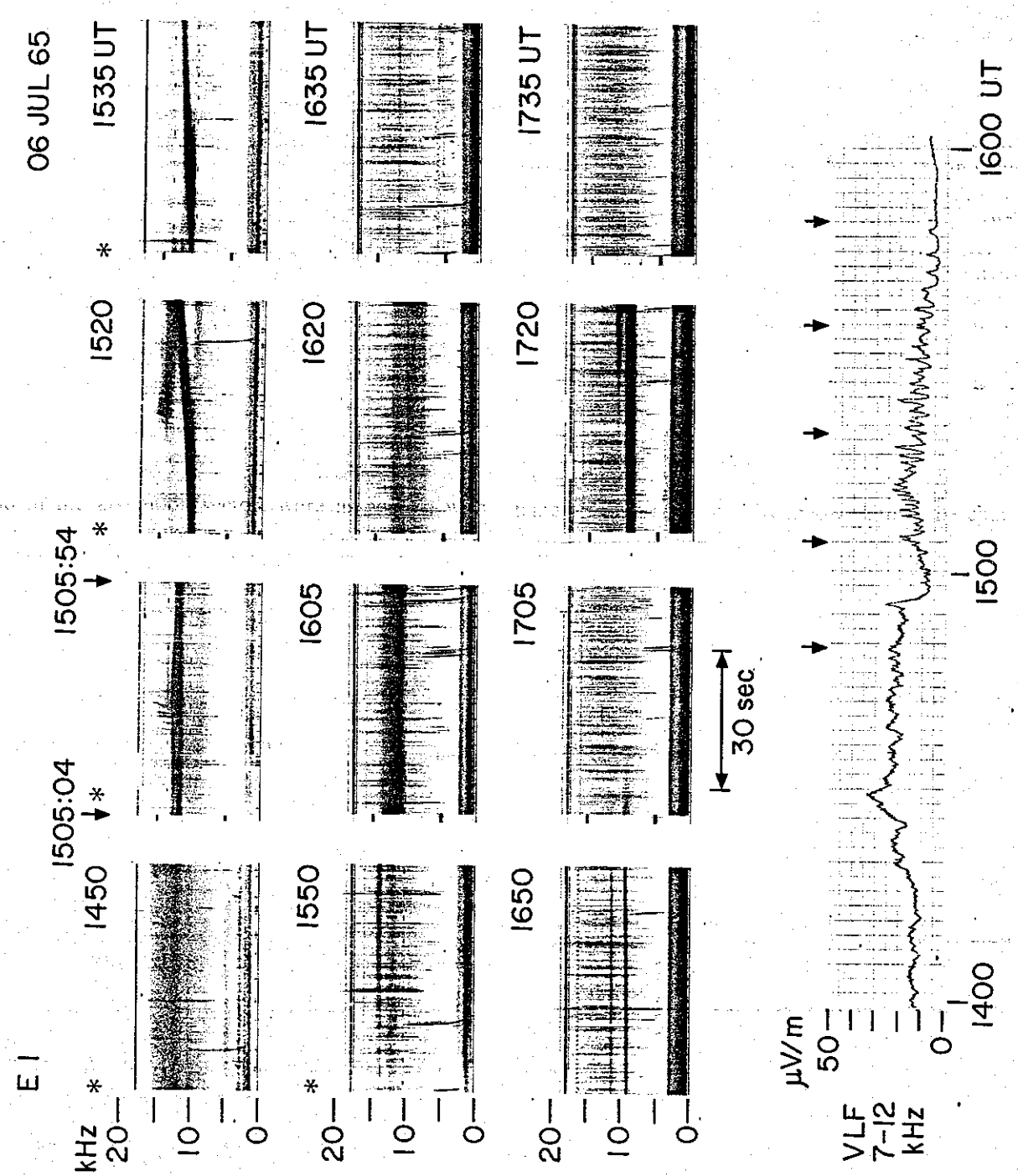


Fig. 2.8. Illustration of VLF noise bands propagating along the outer plasmasphere surface. See text for details.

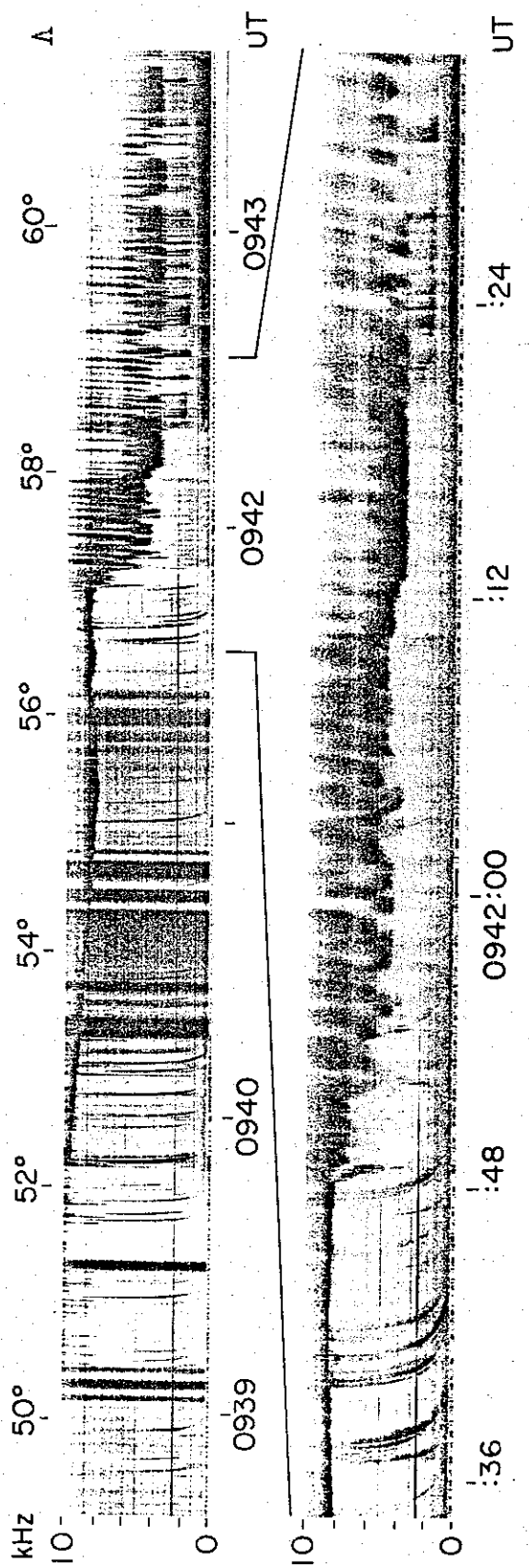


Fig. 2.9. Example of a whistler cutoff and LHR noise breakup observed by the Alouette 1 satellite as it crossed the plasmapause region at ~1000-km altitude [from *Carpenter et al.*, 1968].

bands appeared at intervals of about 1–2 min at this time.

In the upper right half of the 1520 record is an example of a whistler echoing near 15 kHz along the plasmapause. Roughly 20 echoes of the rising upper frequency part of a whistler appear against a diffuse bandlike background.

*Plasmapause-associated wave phenomena observed from satellites.* It is known from ground whistler probing that the plasmapause is particularly well defined during periods of either increasing magnetic activity or moderate but relatively steady magnetic agitation [e.g., *Carpenter and Park*, 1973]. A corresponding statement applies to VLF observations of the plasmapause from polar-orbiting satellites. During such periods there occur abrupt changes in whistler and VLF noise activity at the boundary [*Carpenter et al.*, 1968]. The effects are illustrated in Figure 2.9, which shows broadband VLF spectra telemetered from the Alouette 1 satellite to Byrd, Antarctica, on August 26, 1965. The upper panel shows VLF activity as the satellite moved from about 50° to 62° invariant latitude. The lower panel shows an expanded view of the activity near the plasmapause crossing, which took place at ~0941:48 UT. The crossing is characterized by an abrupt disappearance of whistlers propagating from the conjugate hemisphere. Until 0941:48 UT, whistlers propagating within the plasmasphere appeared at a rate of several per minute. The rate then dropped abruptly; after 0942:03 UT, essentially no such whistlers were seen. Inside the plasmapause at $\Lambda < 57°$ the LHR noise band, which is a characteristic VLF feature on satellites with long electric antennas [*Brice and Smith*, 1964], decreased slowly or remained relatively steady near 8 kHz. This is an indication of relatively normal plasmaspheric conditions. At 0941:48 UT the noise band began to 'break up,' and its apparent lower limiting frequency decreased. This is a characteristic feature of plasmapause crossings; the apparent decrease in the LHR frequency is indicative of passage into a 'light ion trough' [*Taylor*, 1972], where $O^+$ is the dominant ion species. The intensity of the noise activity just beyond the plasmapause is indicated by the automatic gain control action of the receiver, which suppressed the interference line that appeared near 2.4 kHz within the plasmasphere.

Beginning at about 0942:20 UT there appeared a series of impulsive noises which exhibit a lower-intensity cutoff near 2 kHz. Close inspection of these events reveals that they were produced by whistler traces propagating along the outer surface of the plasmapause.

### 2.3. *Magnetospheric Electric Fields*

At altitudes above ~100 km, electrical conductivity in the direction of the geomagnetic field **B** is so large that the electric field component parallel to **B** is negligibly small. (Exceptions may be found at high latitudes where large parallel electric fields are believed to be produced inside electrostatic double layers or in anomalous resistivity regions. Such phenomena, however, are beyond the scope of this chapter.) For many practical purposes, particularly in the plasmasphere, where thermal plasma densities are high, magnetic field lines can be considered equipotentials. If we assume a fixed potential difference between two such field lines, the electric field strength between them should vary in inverse proportion to their separation. Thus electric fields measured anywhere above ~100 km can be mapped up and down along magnetic field lines in a straightforward way.

If we assume perfectly conducting field lines and an electric field **E**, the plasma assumes a bulk flow velocity **v** given by $\mathbf{v} = (\mathbf{E} \times \mathbf{B})/B^2$. The flow is perpendicular to both **E** and **B**. Furthermore, it is flux preserving; as it moves, a tube of ionization changes its volume and shape so as to preserve the amount of magnetic flux threading the tube. Thus field-aligned structures such as whistler ducts should remain field aligned as they undergo **E** x **B** drift. Whistler ducts embedded in the plasma have in fact served as convenient markers to measure cross-$L$ or meridional drift velocities and the associated electric fields. The technique allows measurements of electric fields as small as 0.02 mV/m in the equatorial magnetosphere and has been used since the mid-1960s to study electric field distributions during both magnetic disturbances and quiet times. At middle latitudes the whistler technique offers special advantages over other known methods in terms of both sensitivity and data coverage.

Inside the plasmapause the whistler nose frequency is given by (from section 2.1)

$$f_n = 0.37 f_{Heq} = 1.04 \times 10^{10} B_{eq}$$

if the minimum electron gyrofrequency $f_{Heq}$ and $f_n$ are measured in hertz and the minimum $B$ field $B_{eq}$ is measured in teslas (1 T = $10^9$ γ). A change in $f_n$ can be written in terms of two components:

$$\frac{df_n}{dt} = 1.04 \times 10^{10} \left( \frac{\partial B_{eq}}{\partial t} + \mathbf{v} \cdot \nabla B_{eq} \right) \quad (2.2)$$

The first term represents temporal variations of $B_{eq}$, whereas the second term is due to convection of ducts into regions of different $B_{eq}$. The convection velocity at the equator is given by

$$\mathbf{v} = (\mathbf{E} \times \mathbf{B}_{eq})/B_{eq}^2 \quad (2.3)$$

where **E** is the total electric field including potential ($\nabla \times \mathbf{E}_p = 0$) as well as induced ($\nabla \times \mathbf{E}_i = -(\partial \mathbf{B}/\partial t)$) fields. Combining (2.2) and (2.3) and separating the two types of electric fields, we obtain

$$\frac{df_n}{dt} = 1.04 \times 10^{10} \left[ \frac{\partial B_{eq}}{\partial t} + \mathbf{E}_i \cdot \left( \frac{\mathbf{B}_{eq} \times \nabla B_{eq}}{B_{eq}^2} \right) + \mathbf{E}_p \cdot \left( \frac{\mathbf{B}_{eq} \times \nabla B_{eq}}{B_{eq}^2} \right) \right] \quad (2.4)$$

The first two terms inside the bracket represent effects due to changing magnetic fields and can be significant during storm sudden commencements (ssc) and sudden impulse (si) events [*Park*, 1975]. Whistler observations during such periods have potential applications in studies of the response of the magnetosphere to sudden changes in the solar wind pressure that cause ssc and si. During other times, including storm and substorm periods, the third term dominates, and the observed changes in $f_n$ are interpreted largely in terms of potential electric fields [*Block and Carpenter*, 1974]. In a dipole model a westward electric field $E_w$ in the equatorial plane is then given by

$$E_w = 2.1 \times 10^{-2} \, df_n^{2/3}/dt \quad V/m \quad (2.5)$$

The conventional whistler technique provides no information about the radial component of electric field (north-south component at ionospheric heights). In principle, direction finders can follow the motion of duct exit points and resolve both north-south and east-west components of the electric field. Recent developmental efforts in direction-finding techniques have produced several systems that show promise of fulfilling these expectations [*Bullough and Sagredo*, 1973; *Leavitt*, 1975; *Tsuruda and Hayashi*, 1975].

We now briefly review results on magnetospheric electric fields obtained through the conventional whistler technique.

*Substorm electric fields.* During magnetospheric substorms, electric fields originating at auroral latitudes penetrate deep within the plasmasphere. These fields show complex temporal and spatial variations; however, after many case studies, certain repeatable features begin to emerge. Some features are well established now, while others must still be considered tentative.

One of the well-established features of substorm

electric fields is a westward field that appears in the postmidnight sector [*Carpenter and Stone*, 1967; *Carpenter et al.*, 1972]. This is illustrated by an example in Figure 2.10. The nose frequency and the corresponding path equatorial radius are plotted as functions of time for several different whistler ducts. The vertical scale on the right is linear in $f_n^{2/3}$, so that a constant slope indicates a constant electric field (see (2.5)). A westward field of ~0.3 mV/m appears at the onset of substorm activity at ~0615 UT as indicated by the auroral electrojet (*AE*) index.

In a large number of case studies a westward field, typically of 0.2–0.5 mV/m in the equatorial plane, emerges as a repeatable substorm signature between about 00 and 04 magnetic local time (MLT). These local time boundaries may shift in either direction, depending on individual substorms. The boundary on the midnight side is particularly well defined; prior to ~23 MLT, $E_w$ during substorms may be near zero or slightly negative [*Park and Carpenter*, 1970]. Near 04 MLT a frequently observed feature is a temporal reversal from westward to eastward fields (inward to outward drifts)

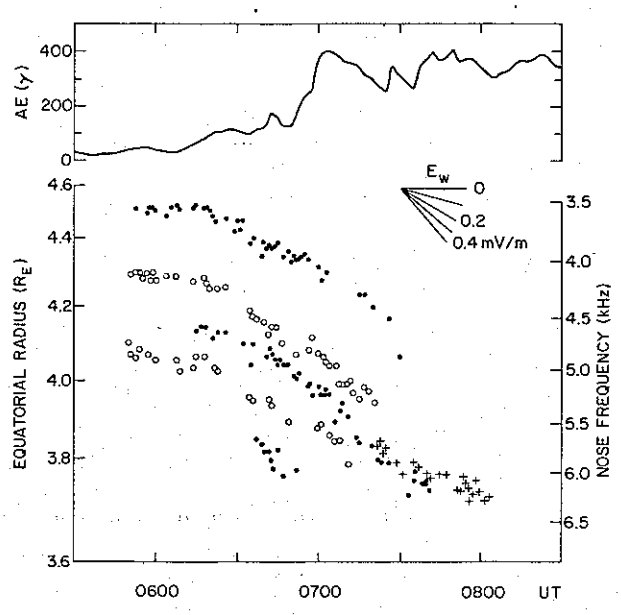


Fig. 2.10. Westward magnetospheric electric fields deduced from drifting whistler ducts. The data points show variations in nose frequency (vertical scale at right) and corresponding equatorial crossing radius (vertical scale at left) as functions of time on July 15, 1965. The whistlers were recorded at Eights, Antarctica, where local magnetic time is ~5 hours behind universal time. Nonlinear vertical scales are used so that a constant slope in the plot would correspond to a constant electric field as indicated in the upper right-hand corner. The curve at the top shows the *AE* index (adapted from *Carpenter and Stone* [1967]).

at the cessation of isolated substorms [*Carpenter et al.*, 1972; *Carpenter and Seely*, 1976]. During prolonged substorm activity, apparently as part of the process by which the worldwide average plasmapause radius is substantially reduced, westward substorm fields and associated cross-$L$ inward drifts tend to persist until ~06–07 MLT [*Carpenter et al.*, 1972].

On the dayside, substorm fields usually have eastward components associated with plasma flow in the generally sunward direction [*Carpenter and Seely*, 1976]. In the dusk sector, eastward fields of the order of 0.2 mV/m in the equatorial plane have been observed to extend as far as 20 MLT [*Park*, 1976*a*]. The present picture is not clear in the dawn sector.

The ionospheric counterpart of the magnetospheric electric fields discussed above is expected to contribute to $F_2$ layer disturbances through the vertical component of **E x B** drift, as was first suggested by *Martyn* [1953]. Experimental evidence for such effects has been found in ionosonde data [*Park and Meng*, 1973; *Park*, 1976*a*].

*'Quiet time' electric fields.* During magnetically quiet periods ($Kp$ = 0–2), magnetospheric electric fields near $L$ = 4 deduced from whistlers show a generally repeatable diurnal pattern. The magnetosphere rarely remains quiescent for several days in succession. However, owing to the extensive time coverage of whistler data, *Carpenter and Seely* [1976] were able to base a description of 'quiet time' electric fields on cases preceded by several days of quiet. The results not only serve as a reference in studying substorm electric fields, but also provide information on the ionospheric dynamo process, another important source of electric fields in the ionosphere and the magnetosphere [e.g., *Matsushita*, 1971].

Figure 2.11 shows the equatorial electric field near $L$ = 4 on two exceptionally quiet days. The curves represent the results of Fourier analysis of 30-min average electric fields. The fields are largest on the dayside, in contrast to fields observed during disturbed times, and in the afternoon-dusk sector their sense is opposite to that of the substorm fields discussed above.

Although the origin of these quiet time fields is not yet known, dynamo winds in the ionosphere may possibly be an important causative factor [*Carpenter and Seely*, 1976]. The whistler results are in general agreement with several of the predictions of dynamo theory [*Maeda*, 1964; *DeWitt and Akasofu*, 1964; *Schieldge*, 1974] and also with dayside inco-

herent scatter radar measurements made at ionospheric heights [*Evans*, 1972].

### 2.4. *Plasma Flow Between the Ionosphere and the Magnetosphere*

The study of plasma flow between the ionosphere and the magnetosphere is complicated by the fact that the two regions are dominated by different ion species: $O^+$ ions in the ionospheric $F$ region up to about 1000 km and $H^+$ ions above that level. $NO^+$ and $He^+$ ions are also present, but at middle latitudes they usually remain minor constituents everywhere at $F$ region heights and above. The term 'protonosphere' is conveniently used to refer to the upper region where $H^+$ is the major ion.

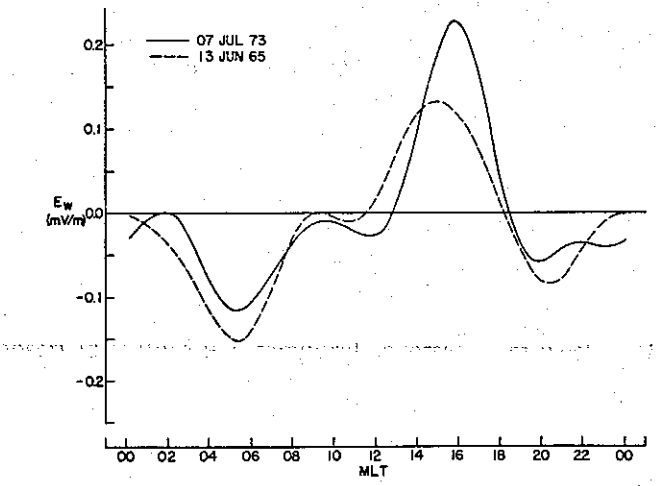


Fig. 2.11. Local time variations of quiet time magnetospheric electric field near $L = 4$ deduced from whistlers on two different days [from *Carpenter and Seely*, 1976].

Figure 2.12 illustrates typical height distributions of electrons and ions at middle latitudes. The transition level is where the dominant ion species changes, while the critical level marks the boundary between the region of chemical control and the region of diffusive control for $H^+$ ions. Below the critical level, $H^+$ density is controlled primarily by the charge exchange reaction $H + O^+ \rightleftarrows H^+ + O$; above the critical level, diffusion dominates over chemical reactions. The corresponding critical level for $O^+$ is below the $F_2$ layer peak.

In order to maintain charge neutrality it is clear that electrons flowing upward from the ionosphere into the protonosphere must be accompanied by an equal number of protons. Since the source of protons is in the chemical equilibrium region, well below the transition level, the upward moving protons must suffer frequent coulomb collisions with the dominant $O^+$ ions before escaping into the protonosphere. This severely impedes the upward plasma flow, and the region between the critical level and the transition level has been called the 'diffusive barrier' [*Hanson and Ortenburger*, 1961]. Theory shows that regardless of how low plasma pressure is in the protonosphere, the upward flux of

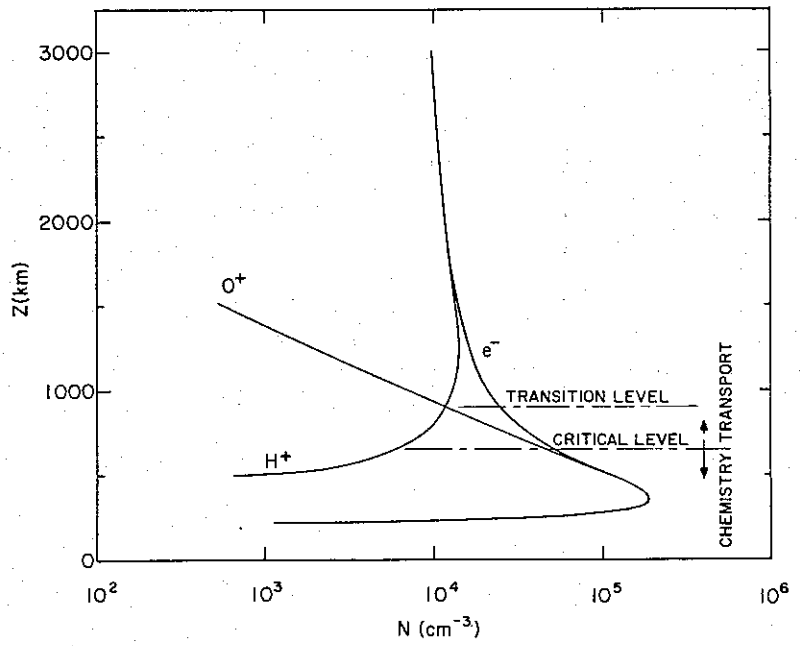


Fig. 2.12. A schematic illustration of electron and ion distributions in the ionosphere.

$H^+$ ions has a well-defined upper limit, determined by the conditions in the diffusive barrier region [*Hanson and Patterson,* 1964; *Geisler,* 1967; *Banks and Holzer,* 1969].

Whistlers provide a unique tool for studying ionosphere-protonosphere coupling. Figure 2.13 illustrates a case in which the daytime filling rate of the protonosphere could be measured by continuously monitoring $f_n$ and $t_n$ for four different ducts (Figures 2.13*a* and 2.13*b*). The $L$ values of the individual ducts remained fairly constant throughout the period of observation (Figure 2.13*c*), but the corresponding tube electron contents increased steadily (Figure 2.13*d*). Since diffusion across magnetic field lines is negligible above 1000 km, the tube content increases can be interpreted in terms of field-aligned flow from the underlying ionosphere. Figure 2.13*d* implies an average upward flux of $3 \times 10^8$ el $cm^{-2}$ $s^{-1}$. These observations were made during a poststorm recovery period when the protonosphere was still depleted. (Compare tube contents in this case with typical values in section 2.5.) Therefore the flux quoted above is probably close to the limiting flux value.

Although upward fluxes of this magnitude may significantly deplete protons in the topside ionosphere, they have little effect on the normal $F_2$ layer, where there is copious production of $O^+$ and electrons by photo-ionization [*Park and Banks,* 1975]. The real significance of these fluxes as far as the $F_2$ layer is concerned lies in the fact that they set an upper limit on how much plasma can return to help maintain the layer at night without depleting the plasmasphere. (The maintenance of the nighttime $F$ layer has been discussed extensively in the literature because of earlier difficulties in explaining the persistence of ionization in the absence of photoionization [*Hanson and Patterson*, 1964; *Yonezawa,*

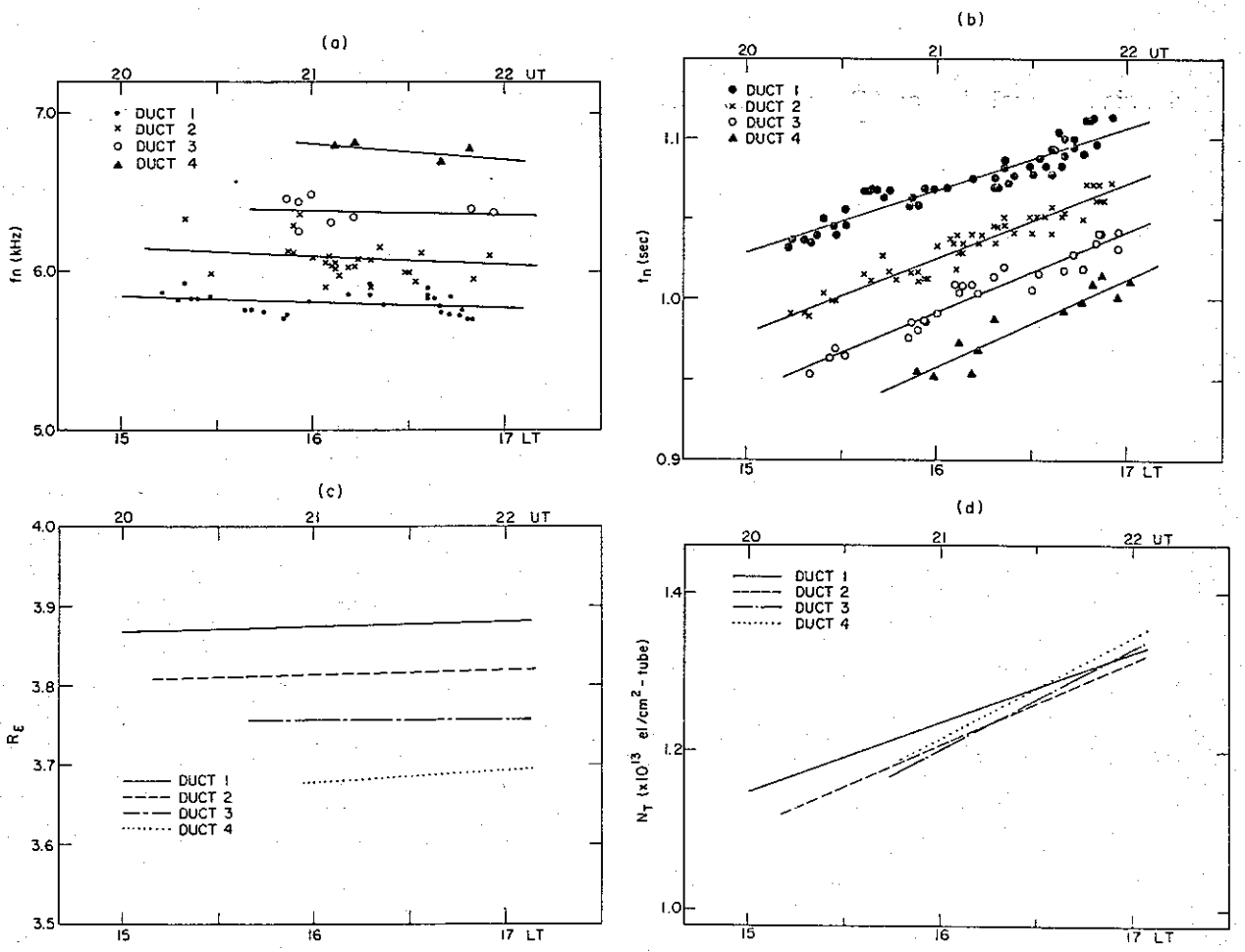


Fig. 2.13. (*a*, *b*) Plots of whistler nose frequency and nose time delay versus time for four different ducts. The whistlers were recorded at Eights, Antarctica, on June 18, 1965. (*c*, *d*) Equatorial crossing radius and electron tube content corresponding to Figures 2.13*a* and 2.13*b* [from *Park*, 1970].

1965; *Stubbe*, 1968; *Titheridge*, 1968].) An upper limit of $3 \times 10^8$ el cm$^{-2}$ s$^{-1}$ is sufficient to allow the plasmasphere to maintain a nocturnal $F$ layer with a peak density of $\geq 10^5$ el/cm$^{-3}$. This is an important factor in explaining ionospheric behavior during long winter nights when the peak density remains constant or even increases slightly. Recent theoretical work shows that the plasmasphere has a strong stabilizing influence on the underlying nighttime $F$ layer; the upper region tends to regulate plasma flow in such a way as to maintain the peak ionospheric density at a certain level [*Park and Banks*, 1974]. This level is determined by plasma pressure in the high-altitude plasmasphere but is remarkably insensitive to conditions at $F$ layer heights.

In the mid-latitude plasmasphere where the flux tube volume is $>10^{10}$ cm$^3$ and the average tube content is $>10^{13}$ el, fluxes of the order of $10^8$ cm$^{-2}$ s$^{-1}$ cannot change plasmaspheric densities significantly on time scales of a day or so. In other words, the plasmasphere cannot follow large diurnal and storm time variations in the underlying ionosphere. This is illustrated in Figure 2.14, where whistler measurements of equatorial density at $L = 4$ (middle panel) are compared with simultaneous $F_2$ layer peak densities over Ottawa. The $L$ value of Ottawa is 3.6; its longitude is close to that of the whistler receiver at Eights. The magnetic storm that started on June 15 (see $Kp$ index above) caused the plasmapause to shrink to $L \simeq 2.5$, reducing the density at $L = 4$ to a level of a few electrons per cubic centimeter. Subsequent recovery was a long process; 5 days were required to reach the monthly median value. The equatorial density continued to increase beyond the median value until June 25, when the plasmasphere was depleted again by a small disturbance, indicated by a rise in the $Kp$ index. The ionosphere was also disturbed during the magnetic storm, but the recovery was much faster. Equatorial densities are shown in greater detail from June 18 through June 22 to reveal small diurnal fluctuations superimposed on an almost linear increase. These variations are consistent with a daytime upward flux of $3 \times 10^8$ cm$^{-2}$ s$^{-1}$ and a nighttime downward flux of $1.5 \times 10^8$ cm$^{-2}$ s$^{-1}$ [*Park*, 1970]. It is clear that the plasmasphere acts as a large-capacity reservoir with a much longer response time than the underlying ionosphere. Evidence from the June 25 disturbance indicates that a rapid dumping of plasmaspheric plasma into the underlying ionosphere caused the decrease in equatorial density and simultaneous enhancements in $N_mF_2$ [*Park*, 1973]. Such effects are important in understanding the complex ionospheric storm.

To summarize, the diffusive barrier limits upward plasma flow to a level that does not allow the plasmasphere to follow large diurnal variations in the ionosphere. Upward fluxes are too small to deplete the daytime $F$ layer significantly but are sufficiently large to replenish the plasmasphere, which acts as an important source of plasma for the $F$ layer at night and during geomagnetic disturbances. The results of recent theoretical modeling are in agreement with this picture of ionosphere-

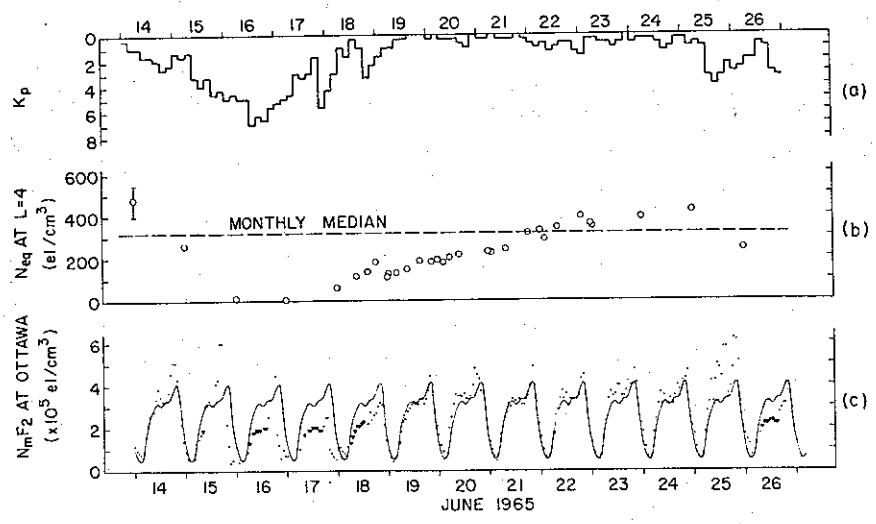


Fig. 2.14. (*a*) The 3-hour $Kp$ index for the period June 14–26, 1965. (*b*) Equatorial electron density at $L = 4$ deduced from whistlers recorded at Eights, Antarctica. (*c*) $F_2$ layer peak density over Ottawa. The solid curve represents the monthly median behavior, and the triangles with the apex pointing downward represent upper limits [from *Park*, 1970].

plasmasphere coupling [*Park and Banks*, 1974, 1975; *Murphy et al.*, 1975].

### 2.5. *Electron Density Variations in the Plasmasphere*

*Storm and substorm effects.* The protonosphere is generally depleted during magnetic storms and substorms and then recovers gradually by filling from the underlying ionosphere. An example of this was already seen in Figure 2.14. Details of the depletion process are not well understood, but there may be several different mechanisms involved. Figure 2.15 illustrates schematically how the equatorial electron density profile changes during a disturbance. The plasmapause is displaced inward, probably owing to enhanced magnetospheric convection that carries plasma to regions of 'open' geomagnetic field lines where it can escape into interplanetary space or into the geomagnetic tail region. In addition, densities inside the plasmapause are often depressed, indicating that large amounts of plasma can be dumped into the ionosphere during magnetic disturbances.

The recovery time of the plasmasphere following storm time depletion depends on how fast plasma can flow upward from the ionosphere as well as on the volume of plasmaspheric tubes to be filled. Since the tube volume increases roughly as $L^4$ while the filling flux remains relatively constant with $L$, the recovery time is a strong function of $L$ value. This can be clearly demonstrated by the $L$ dependence of the recovery behavior following the magnetic storm of Figure 2.14. Figures 2.16*a* and 2.16*b* show tube content and equatorial electron density profiles, respectively, on eight consecutive nights, June 18–25, 1965. The magnetic storm of June 15–17 moved the plasmapause inward to $L \simeq 2.5$. During recovery, daytime filling fluxes exceeded nighttime draining fluxes, so that a net nightly gain of $5 \times 10^{12}$ el in tube content was realized until the tube content reached a well-defined saturation level. At this level the plasmasphere is in equilibrium with the underlying ionosphere over a 24-hour period. The recovery time, or the time required to reach saturation, varied from ~1 day at $L = 2.5$ to ~8 days at $L = 4$.

Because of these long recovery times the plasmasphere usually consists of two distinct regions, an inner plasmasphere, which is in equilibrium with the underlying ionosphere over a 24-hour period, and an outer plasmasphere, which is still recovering from the previous disturbance; these two regions may be referred to as the 'saturated plasmasphere' and the 'unsaturated plasmasphere,' respectively, with the understanding that the term saturated is used only in a diurnal average sense. Although most dramatic depletions of the plasmasphere occur during periods of intense substorm activity such as the main phase of a magnetic storm, moderate substorms involving $Kp = 4$ or less also produce significant effects. The average frequency of such moderate substorm activity is less than 8 days, so that the plasmasphere beyond $L = 4$ very rarely, if ever, reaches saturation. The dynamic state of the outer plasmasphere is reflected in large day-to-day

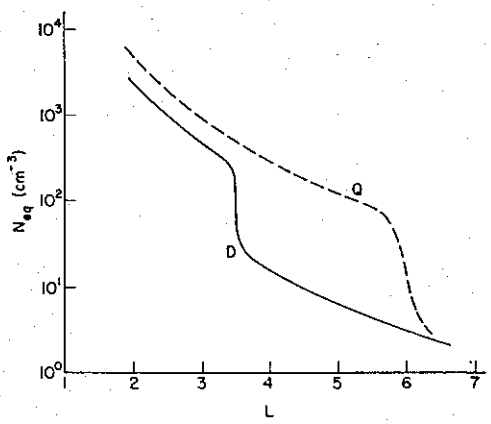


Fig. 2.15. A schematic illustration of equatorial electron density profiles under quiet (Q) and disturbed (D) conditions [from *Park*, 1974].

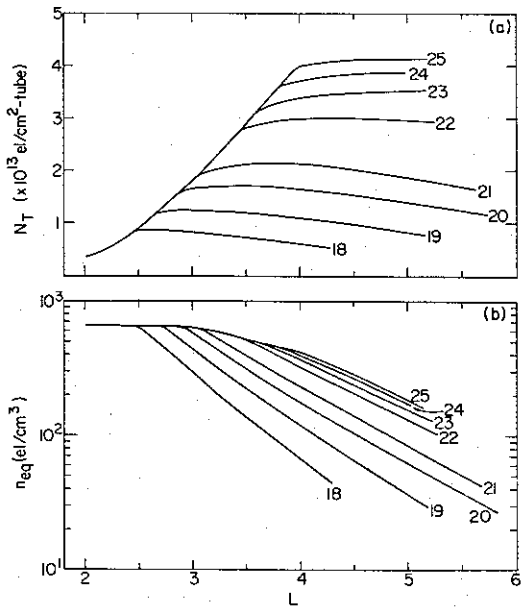


Fig. 2.16. (*a*) Nightly tube content and (*b*) equatorial density profiles deduced from whistlers recorded at Eights, Antarctica, during an 8-day recovery period following a major geomagnetic storm. The numbers indicate UT days in June 1965 [from *Park*, 1974].

density fluctuations that overshadow systematic variations with solar cycle, season, and local time.

The picture described above can also be seen in the average behavior of the plasmasphere illustrated in Figure 2.17. This behavior was determined from whistlers recorded at Eights Station during the month of June 1965. Several representative whistler trains of high quality were chosen from each day's recordings. These events were analyzed to obtain daily tube content and equatorial density profiles, which were then scaled at intervals of $0.25L$. The circles in the figure represent monthly median values, and the vertical bars represent the upper and lower quartile values. The average behavior of the plasmasphere strongly reflects the slow $L$-dependent recovery process depicted in Figure 2.16.

Figures 2.18*a* and 2.18*b* show scatter plots of electron tube content and equatorial electron density, respectively, as functions of $L$ value, deduced from selected high-quality whistlers recorded at Siple during the month of June 1973. Over 3000 whistlers were used. Three important features can be identified in the figure: (1) well-defined upper limits of both tube content and equatorial density; (2) general clustering of data points somewhat below the upper limits; and (3) presence of some data points at relatively low levels, well separated from the majority. The low content and density points come from whistlers propagating outside the plasmapause. The first two features mentioned are consistent with the concept of a saturation level that is rarely reached in the outer plasmasphere.

*Large-scale irregularities.* Figures 2.19 and 2.20 show two types of large-scale density irregularities frequently observed in the plasmasphere. In Figure 2.19 the irregularity takes the form of a pronounced

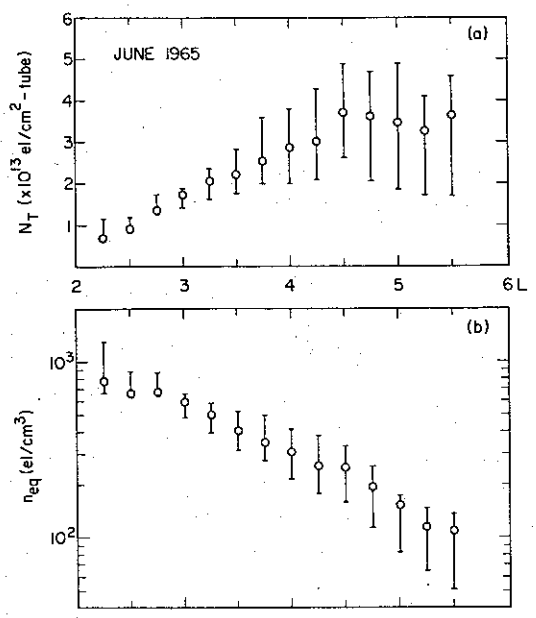


Fig. 2.17. Monthly median values of (*a*) tube content and (*b*) equatorial density deduced from whistlers recorded at Eights, Antarctica, during June 1965. The bars indicate upper and lower quartiles [from *Park*, 1974].

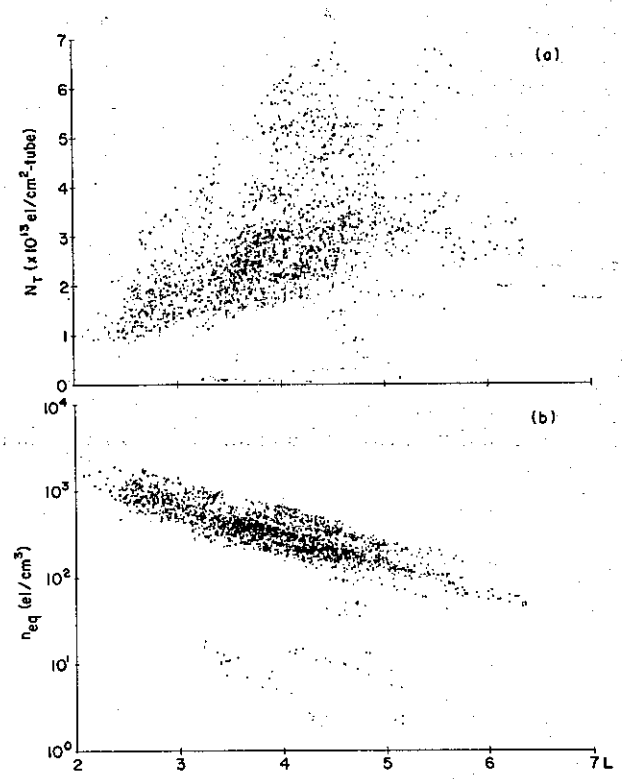


Fig. 2.18. Scatter plots of (*a*) electron tube content and (*b*) equatorial electron density versus $L$. Each plot has over 3000 data points obtained from whistlers recorded at Siple, Antarctica, during the month of June 1973.

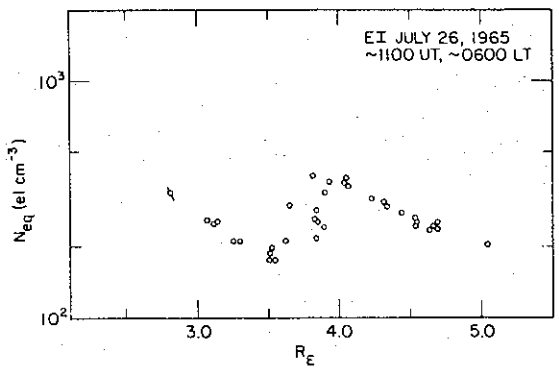


Fig. 2.19. Equatorial electron density versus equatorial radius deduced from Eights whistlers [from *Park and Carpenter*, 1970].

density peak near $L = 4$. Figure 2.20 was interpreted by *Park and Carpenter* [1970] in terms of three density regimes separated in longitude by sharp boundaries within the Eights whistler receiver viewing range of ±15°. Sharp longitudinal variations were also observed outside the plasmapause by *Sagredo and Bullough* [1973], who applied the goniometer technique to whistlers received at Halley Bay. Such structures may be produced by brief substorm activity that affects localized regions of the magnetosphere. Subsequent convection activity tends to further complicate the picture by mixing flux tubes with different plasma content [*Park and Carpenter*, 1970].

*Annual variations*. Figure 2.21 compares monthly median values of $N_T$ and $n_{eq}$ for June 1965 (reproduced from Figure 2.17) with the median values for November and December 1964. All the whistlers used in Figure 2.21 were recorded at Eights Station. The November and December densities are 1.5–3 times larger than the June values, the ratio increasing with decreasing $L$ values. Annual density variations in the plasmasphere have been known since the early days of whistler research [*Helliwell*, 1961; *Smith*, 1961*b*; *Carpenter*, 1962; *Corcuff*, 1962], but they still remain unexp ained. A recent discussion of this problem can be found in a paper by *Park* [1974].

*Solar cycle variations*. Figure 2.22 shows the median values of $n_{eq}$ for the month of June in 1959, 1965, and 1973. June 1959 was near sunspot maximum (annual mean sunspot number $R = 159$), whereas both June 1965 ($R = 15$) and June 1973 ($R = 38$) were near sunspot minimum. The whistler data for 1959, 1965, and 1973 came from Byrd, Eights, and Siple stations, respectively. All three stations are within 1 hour in geomagnetic local time. Evidently, plasmaspheric densities do not depend strongly on sunspot cycle beyond $L \simeq 3$.

*Diurnal variations*. It is clear from the foregoing discussion that diurnal variations in plasmaspheric density should be small in comparison with day-to-day variations due to storms and substorms. If we take a daytime upward flux of $3 \times 10^8$ el cm$^{-2}$ s$^{-1}$ at $L = 4$, the total gain in plasmaspheric tube content over a 12-hour period would be $1.3 \times 10^{13}$, roughly 30% of the average tube content. Systematic variations of this magnitude are difficult to isolate in the data, illustrated in Figure 2.23. Whistlers recorded at Siple during June 1973 were di-

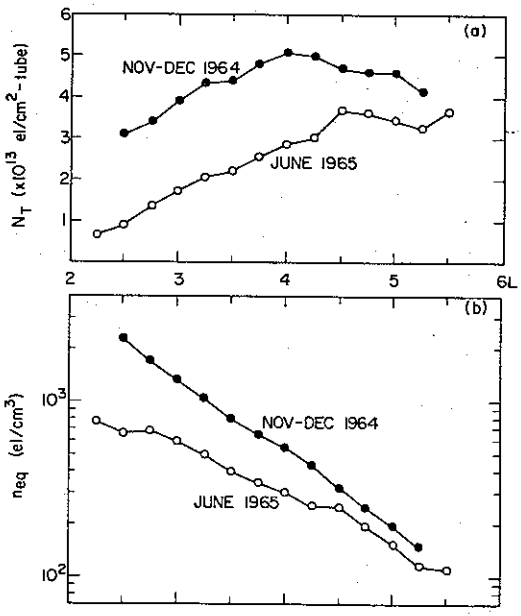


Fig. 2.21. Annual variations in (*a*) electron tube content and (*b*) equatorial electron density. The data points are median values obtained from whistlers recorded at Eights, Antarctica [from *Park*, 1974].

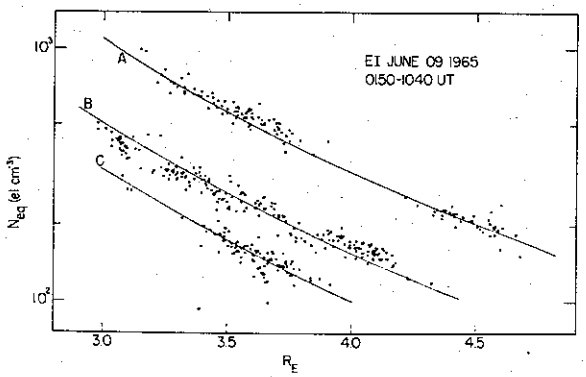


Fig. 2.20. Equatorial electron density versus equatorial radius. The three density levels are interpreted in terms of longitudinal variations within the viewing range of Eights Station [from *Park and Carpenter*, 1970].

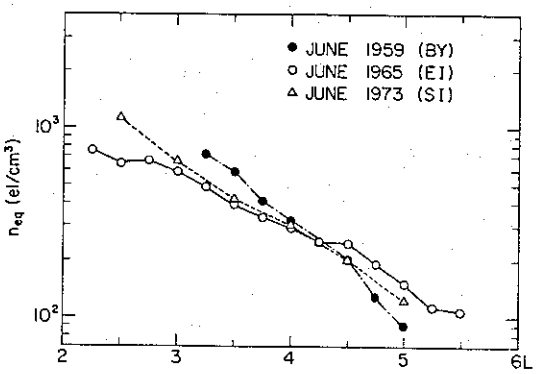


Fig. 2.22. Comparisons between equatorial electron densities near sunspot maximum (1959) and sunspot minimum (1965 and 1973). The data points are monthly median values based on whistlers recorded at Byrd (BY), Eights (EI), and Siple (SI).

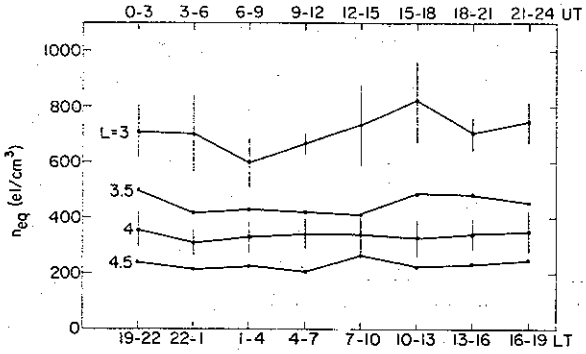


Fig. 2.23. Diurnal variations in equatorial electron density for $3 \leq L \leq 4.5$. The data are based on whistlers recorded at Siple, Antarctica, during the month of June 1973. Dots represent the mean values, and vertical bars represent the magnitude of one standard deviation.

vided into eight 3-hour bins, and the average equatorial densities deduced from them have been plotted for $3 \leq L \leq 4.5$. The vertical bars represent the magnitude of one standard deviation at $L = 3$ and 4. It is apparent that diurnal variations are not prominent features of electron density within the plasmasphere. However, diurnal variations in terms of percentage should be much larger outside the plasmapause, where densities are lower by factors of 10–100.

## 3. VLF EMISSIONS

Energetic electrons in the 100-eV to 100-keV range give rise to a great variety of VLF noises or emissions in the magnetosphere. These have acquired such names as 'chorus,' 'hiss,' and 'periodic emissions.' Under certain conditions, such as propagation within a whistler duct, emissions can penetrate the ionosphere and be observed on the ground. A monograph by *Helliwell* [1965] contains an extensive collection of spectrograms illustrating various types of emissions recorded at ground stations. Since it is not possible to review all of these emission types here, we will discuss only a few highlights of recent research.

VLF emissions may be divided into two broad categories according to their spectral characteristics. The first category covers discrete frequency emissions such as chorus, while the second category includes broadband emissions such as auroral hiss. This distinction helps to emphasize the differences between the quasi-coherent wave trains of discrete emissions and the incoherent noiselike waves in broadband events. The forces experienced by energetic electrons encountering these waves must be correspondingly different, and different mechanisms and regions of generation are usually attributed to the two emission types.

### 3.1. *Discrete Emissions*

Discrete emissions are believed to be generated near the equatorial plane in the magnetosphere by trapped energetic electrons through a cyclotron resonance instability. Although the fundamental importance of these emissions in magnetosphere-ionosphere dynamics was recognized long ago, quantitative studies of their generation process have been complicated by the transient and highly nonlinear nature of the emission process. These difficulties and the general desire to understand the microscopic aspects of wave-particle and wave-wave interactions helped to motivate the establishment of controlled wave injection experiments at Siple Station. The results of these experiments and their contributions to our understanding are discussed in chapter 5.

Emissions may be generated spontaneously or stimulated by other whistler mode waves entering the generation region. The threshold of instability for stimulated emissions is apparently much lower than that for spontaneous emissions; a weak signal entering the magnetosphere from below can initiate and control the emission activity in an otherwise quiescent situation. Important sources of such input signals are lightning, VLF transmitters, and electrical power transmission lines.

Figure 3.1 shows two examples of whistler-triggered emissions. In the upper panel, emissions start at the upper cutoff frequency of several triggering whistler components. This frequency is approximately one half of the minimum electron gyrofrequency along the whistler path (see section 2.1). Triggering at the upper whistler cutoff frequency is a frequently observed feature of whistler data. A preference for half-gyrofrequency triggering was also demonstrated in studies of emission activity triggered by VLF transmitters [*Carpenter*, 1968; *Carpenter et al.*, 1969]. The lower panel in Figure 3.1 illustrates the less common case in which an emission is triggered by the low-frequency end of a whistler.

It is well known that VLF transmitter signals propagating in the whistler mode also trigger strong emissions. Under favorable conditions an Omega navigational transmitter radiating only 100 W can trigger emissions as strong as any naturally occurring emissions [*Kimura*, 1968]. Emission activity stimulated by transmitter signals depends on a number of factors including pulse length, frequency, and radiated power as well as conditions in the ionosphere

and magnetosphere. These factors are being investigated by using a flexible experimental transmitter at Siple.

It was discovered recently that radiation from the power distribution system in Canada leaks into the magnetosphere with sufficient intensity to stimulate emissions and to interact strongly with other whistler mode waves, as in the case of VLF transmitter signals [*Helliwell et al.*, 1975]. (Also see the discussion in section 5 of chapter 5.) Presumably, the same phenomena also occur in other major industrial areas of the world. Power line induced emissions are particularly strong immediately following geomagnetic disturbances and are sometimes the strongest VLF waves emerging from the middle magnetosphere in the 1- to 10-kHz frequency range [*Park*, 1976*b*]. These waves scatter the pitch angles of trapped energetic electrons and cause some of the electrons to precipitate into the lower atmosphere. Thus power line radiation appears to play an important role in the decay of energetic electrons injected during geomagnetic storms and substorms.

Figure 3.2 shows two examples of power line induced emissions recorded at Eights Station during the recovery phase of a magnetic storm. In the upper panel, broad line radiation is strongly modulated in intensity at the two-hop whistler delay period. The bottom panel shows another example in which emissions starting at different frequencies merge to form continuous rising-tone structures. Strong intensity modulation at the two-hop delay period is also evident here.

Amplitude measurements of triggered emissions show that the triggering input signal may be about 30 dB below the output signal [*Stiles and Helliwell*, 1975]. Furthermore, controlled transmitter experiments have shown that weak transmitter signals, barely detectable on conventional spectrograms, can control the behavior of other much stronger signals by cutting them off, enhancing their intensity, or changing their frequency [*Helliwell and Katsufrakis*, 1974]. This suggests the possibility that many (or all) discrete emissions that appear to be generated spontaneously are in fact controlled by weak power line radiation continuously leaking into the magnetosphere.

Emissions can be suppressed as well as initiated by other whistler mode waves. For example, *Ho* [1973] found that whistlers sometimes suppress periodic and quasi-periodic (QP) emissions propagating in the same whistler ducts. Figure 3.3 shows a case of QP emissions suppressed by a train of whistler echoes. Ho also found that whistlers can modify the fine structure of QP emissions or tempo-

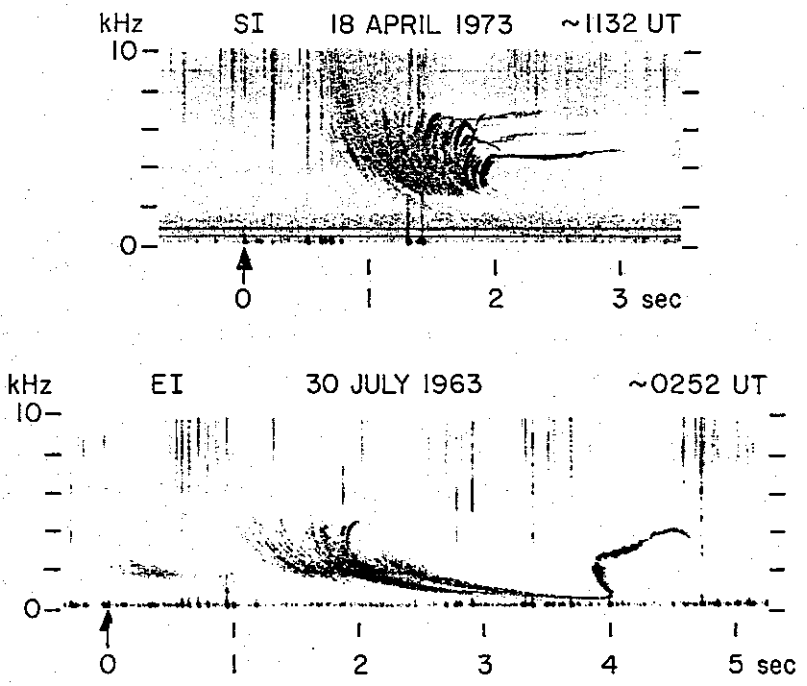


Fig. 3.1. Two different types of emissions triggered by whistlers. In the upper panel, emissions are triggered at the upper cutoff frequency or near one half of the minimum electron gyrofrequency along the whistler paths. The lower panel shows an emission triggered by the low-frequency tail of a whistler.

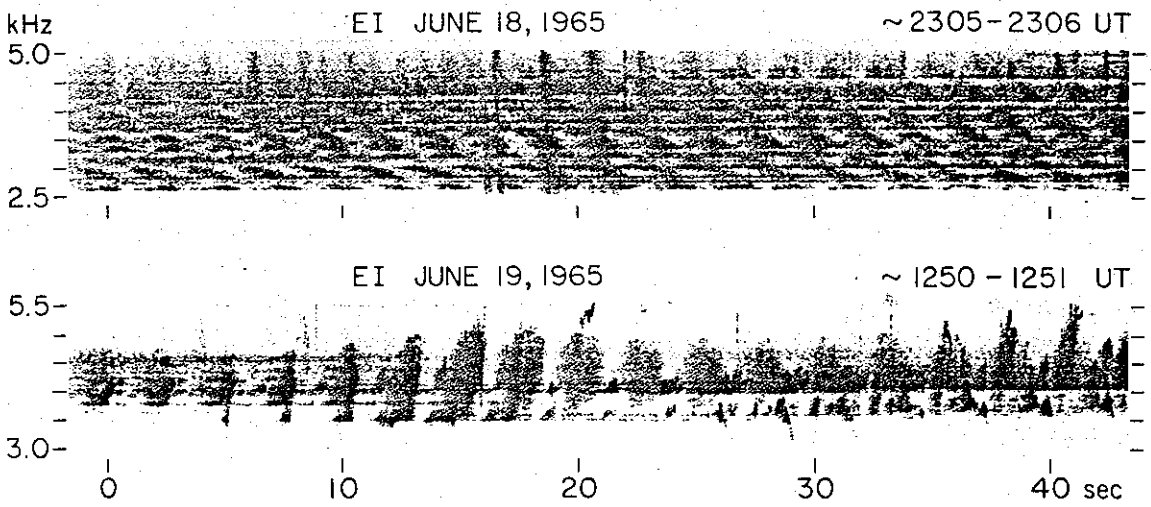


Fig. 3.2. Two examples of magnetospheric emissions recorded at Eights, Antarctica. They are believed to have been stimulated by radiation from electrical power transmission lines in eastern Canada [from *Park*, 1976*a*].

rarily lengthen the QP period. Another example of emission suppression by whistlers is shown in Figure 3.4. The line emissions, spaced 120 Hz apart, are believed to be stimulated by power line radiation. Whistler echo trains starting at 20 and 30 s suppress the power line induced line emissions between ~4.5 and 5.5 kHz. Variable frequency emissions above ~5.5 kHz are also suppressed by the whistler train starting at 20 s. Details of the suppression mechanism are not well understood, but presumably it involves interference by whistlers in the electron phase-bunching process that is required to sustain the emission generation.

### 3.2. *Auroral Hiss*

Energetic electrons precipitating in the auroral zone produce strong VLF radiation known as auroral hiss. Close association between VLF hiss and visible aurora was reported as early as 1933 [*Burton and Boardman*, 1933] and was a topic of great interest during the early antarctic expeditions, as is discussed in chapter 9. More recently, *Morozumi*

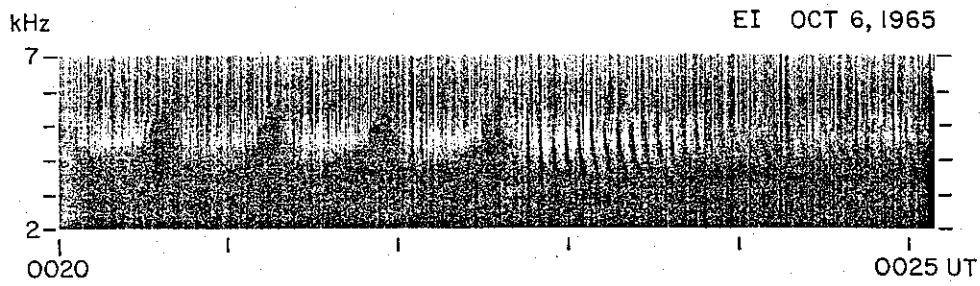


Fig. 3.3. An example of quasi-periodic emissions being suppressed by whistlers.

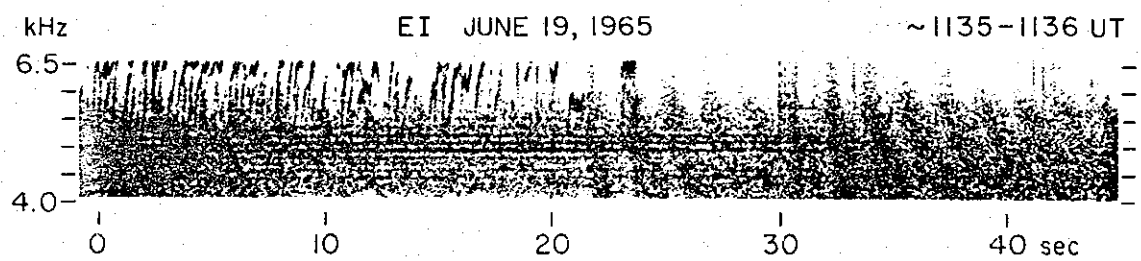


Fig. 3.4. An example of power line induced magnetospheric emissions being suppressed by two whistler echo trains starting at 20 and 30 s.

*and Helliwell* [1966] made detailed studies of hiss activity at Byrd Station during successive phases of magnetospheric substorms, and *Oguti* [1975] used a sophisticated auroral television system with a soundtrack at Syowa Base to correlate hiss bursts with various types of auroral forms.

Auroral hiss generally appears as broadband noise extending from a few kilohertz up to ~100 kHz. This noiselike radiation is clearly distinguished from the coherent discrete frequency emissions discussed in section 3.1. The two types of emissions are believed to involve fundamentally different wave-particle interaction mechanisms, as will be discussed later.

Attention has been focused on special types of auroral hiss that show fine structure in amplitude and spectral characteristics, since they offer better opportunities for correlation with particle, optical, and other measurements which may lead to a better understanding of the generation process. One example is hiss bursts of ~0.1- to 1-s duration that *Oguti* [1975] found to be closely associated with rapid motions and intensity variations of visible aurora.

Another special type of hiss is the 'hissler,' so called because it tends to occur at times and locations common to auroral hiss while also exhibiting a whistlerlike falling tone form on spectrographic records [*Ungstrup and Carpenter*, 1974]. A distinctive feature of the hissler is its quasi-periodicity. Hisslers often appear in minute-long sequences with spacing between individual bursts of the order of 2 s at a given frequency.

Figure 3.5 shows frequency (0–10 kHz) versus time records of hisslers recorded at Byrd (upper panel) and Vostok (lower panel). A 10-s interval is marked below each of the panels. On the upper record the sloping noise elements initially appear against an intense background of broadband noise, and there is a gradual change in the lower cutoff frequency of the elements with time. On the lower record the activity is more complex, exhibiting much fine structure and an apparent increase with time in the lower cutoff frequency of some of the noise elements. In the upper record a typical separation between elements is 2 s; in the lower record it is about 3 s.

From observations at several antarctic stations such as Byrd, Vostok, and Plateau and from polar satellite records it was tentatively concluded that localized centers of hissler activity are regularly present above the ionosphere. These centers may be active for periods of several hours at a time.

*Siren* [1972, 1975] identified another form of hissler, which he called the 'fast hissler.' The fast hissler is a relatively rare phenomenon and is distinguished from other hisslers by its small dispersion. It tends to occur in isolated bursts during the breakup phase of auroral substorms. Siren suggested the possibility that fast hisslers are generated by electrons accelerated in electrostatic double layers in the topside ionosphere [e.g., *Block*, 1972].

Auroral hiss has also been studied extensively by using a number of polar-orbiting satellites [*Gurnett*, 1966; *Jørgensen*, 1968; *Barrington et al.*, 1971; *Gurnett and Frank*, 1972; *Laaspere and Hoffman*,

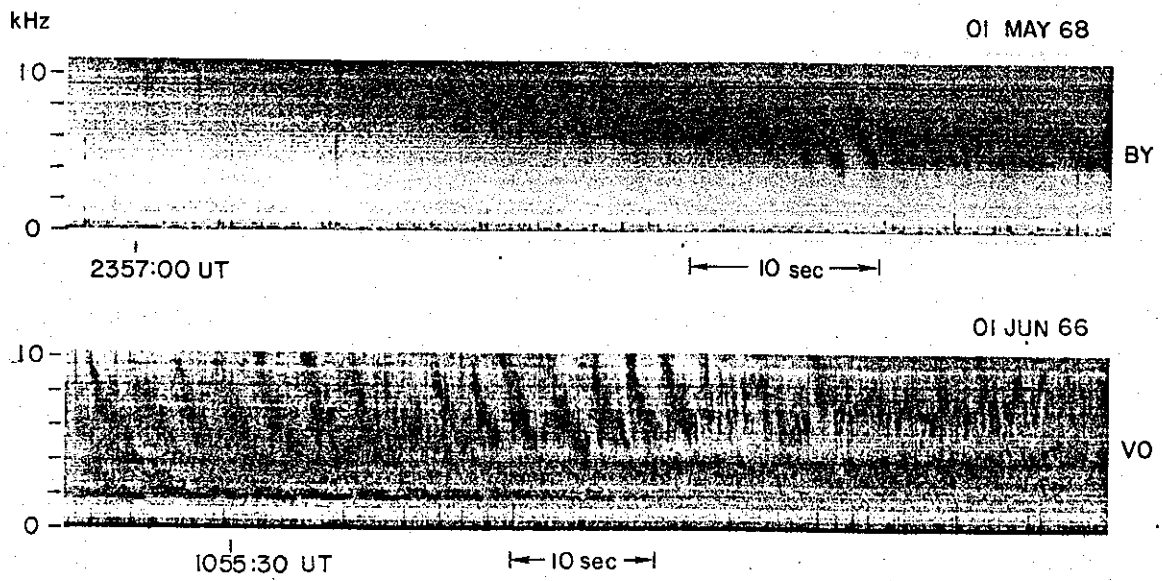


Fig. 3.5. VLF spectra illustrating hisslers observed at Byrd ($\Lambda = 70°$) and Vostok ($\Lambda \sim 86°$).

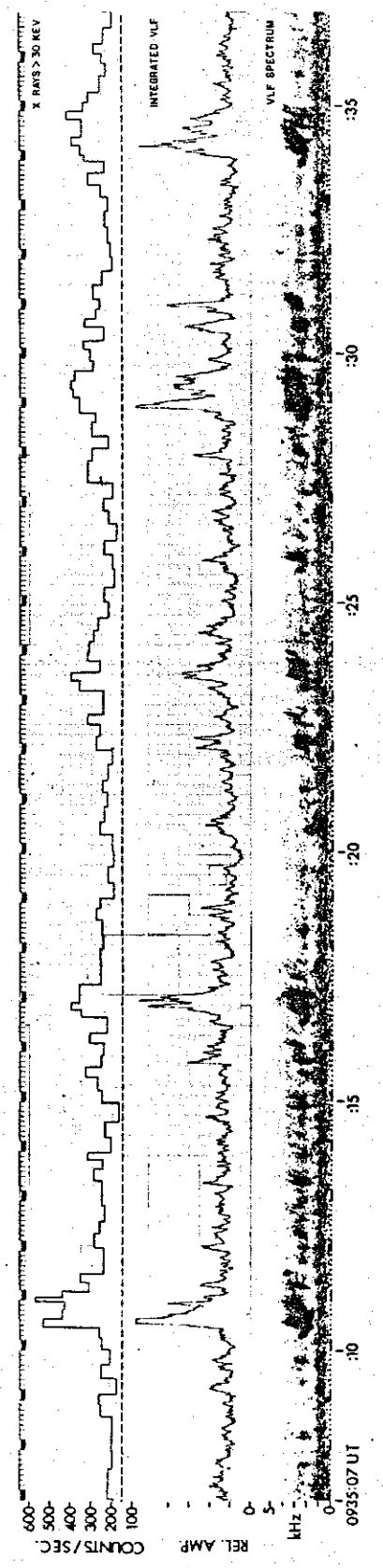


Fig. 3.6. A 30-s segment of simultaneous recordings of (top) the X ray count rate for $E > 30$ keV, (middle) the integrated VLF amplitude from 0.6 to 5 kHz, and (bottom) the VLF spectrum from 0 to 5 kHz recorded at Siple, Antarctica, on January 2, 1971. The dashed line in the top panel refers to the cosmic ray background level of 175 counts/s [from *Rosenberg et al.*, 1971].

1976]. Satellite records frequently show distinct saucer- or V-shaped structures in the frequency-time plane that are believed to be the result of satellite motion with respect to spatially localized generation regions [*Smith*, 1969; *James*, 1976].

In addition to VLF hiss that propagates in the whistler mode, satellite-borne receivers have also detected strong radiation at frequencies much above the electron gyrofrequency and originating from the auroral zone during active periods. (Recall that whistler mode propagation is possible only below the electron gyrofrequency.) This type of radiation has been called 'high-pass noise' [*Dunckel et al.*, 1970] or 'terrestrial kilometric radiation' [*Gurnett*, 1974].

A number of authors have discussed the generation of VLF auroral hiss by the incoherent Cerenkov mechanism [*Jørgensen*, 1968; *Lim and Laaspere*, 1972; *Taylor and Shawhan*, 1974; *Maggs*, 1976]. It is generally agreed that this mechanism alone cannot explain the observed wave intensity; some degree of coherence and amplification appear to be necessary. Unlike discrete emissions, which interact with particles through transverse (or cyclotron) resonance, hiss amplification is believed to involve longitudinal resonance between the electron velocity component along the geomagnetic field and the wave electric field in the same direction (see chapter 5, section 3).

### 3.3. *Wave-Induced Particle Precipitation*

The previous sections treated the wave aspects of wave-particle interactions. The corresponding particle effects are also important, one of them being pitch angle scattering and consequent precipitation into the lower ionosphere. Particle precipitation in turn causes a variety of ionospheric effects including enhanced ionization, heating, optical emissions, and bremsstrahlung X rays.

Figure 3.6 shows an example of clear association between VLF emissions and X ray bursts. The X ray data were obtained from a balloon flying at 30-km altitude over Siple, while the VLF recording was made on the ground at Siple. Detailed analysis showed that the VLF emissions were triggered by whistlers propagating outside the plasmapause and that their correlation with X ray bursts was consistent with the precipitation of ~30-keV electrons through a cyclotron resonance interaction [*Rosenberg et al.*, 1971]. The results of this coordinated experiment are discussed in greater detail in chapter 3, section 5.

Another wave-induced particle precipitation ef-

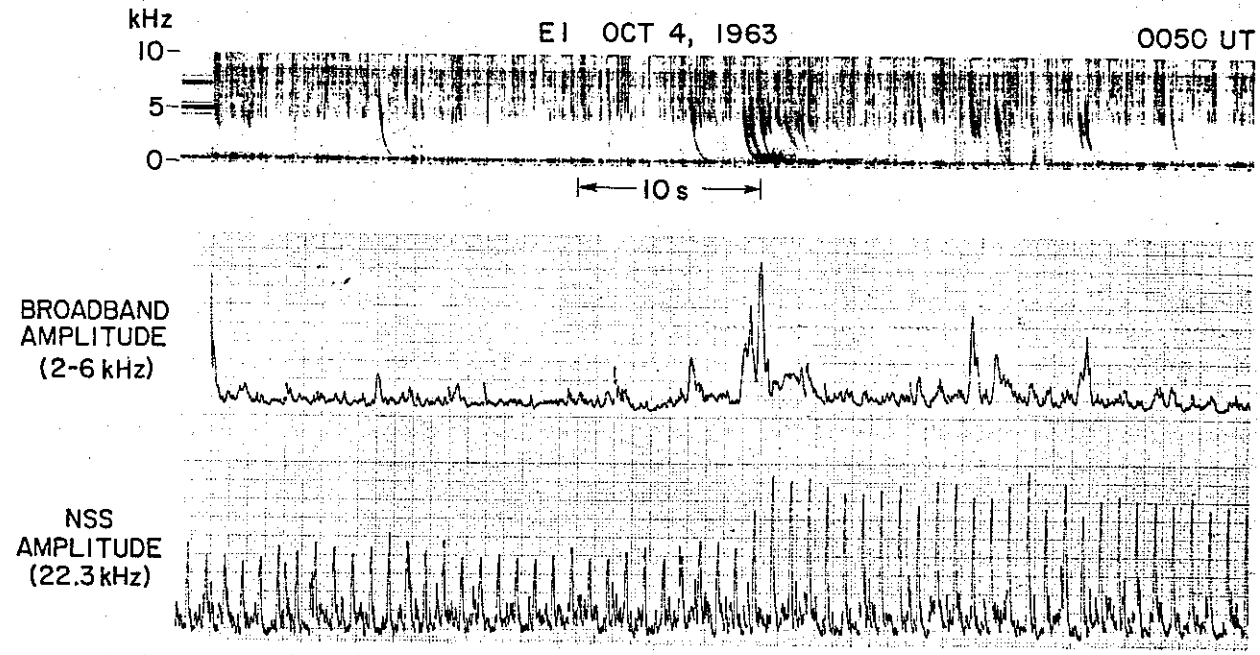


Fig. 3.7. (Top) VLF spectra, (middle) integrated VLF amplitude from 2 to 6 kHz, and (bottom) NSS pulse transmissions observed at Eights, Antarctica [from *Helliwell et al.*, 1973].

fect is illustrated in Figure 3.7. A whistler received at Eights (upper and middle panels) coincides with a sudden increase in the amplitude of VLF signals propagating from the transmitter NSS at Annapolis, Maryland, to Eights. The causal chain linking the two events can be explained with the aid of Figure 3.8. A lightning discharge in the northern hemisphere excites a whistler traveling along a magnetospheric path to the receiver (R) at Eights. During its passage through the wave-particle interaction region near the equator the whistler interacts with counterstreaming energetic electrons and causes some of them to precipitate into the lower ionosphere in the northern hemisphere. Some of the perturbed particles are backscattered and are precipitated in the southern hemisphere. The patches of enhanced ionization thus created at ~90-km altitude (assuming nighttime conditions) cause perturbations in signals propagating in the earth-ionosphere wave guide. The amplitude perturbations can be negative as well as positive. The recovery time of a perturbation is of the order of 30 s and is related to the electron loss rates in the lower ionosphere.

These results are in agreement with other evidence that most of the ionization in the nighttime *D* region ionosphere can be attributed to particle precipitation from the magnetosphere [*Potemra and Zmuda*, 1970]. Wave-induced precipitation offers the possibility of conducting controlled modification experiments in the lower ionosphere [e.g., *Bell*, 1976].

## 4. FUTURE DIRECTIONS

The whistler method has proved to be a powerful means of probing the magnetosphere; the method has provided much of our presently available information on plasmasphere-plasmapause dynamics. What we have learned from whistlers also serves to define important unanswered questions clearly and to identify improvements in experimental and theoretical methods that are needed for future progress. For example, we now have only a fragmentary picture of the global plasma flow pattern during geomagnetic disturbances. A closely related question is how the plasmapause shrinks during disturbed periods and what happens to the large amounts of plasma that disappear from the plasmasphere. It is

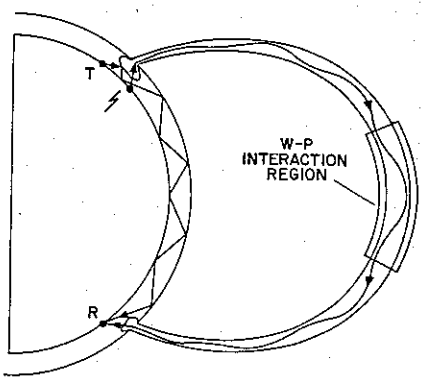


Fig. 3.8. A schematic illustration of how a whistler might produce perturbations in the subionospheric propagation of VLF transmitter signals by precipitating energetic electrons.

clear that in order to answer these questions we need simultaneous observations at multiple stations spaced in longitude.

The present whistler technique provides information about plasma drift only in the meridional direction. This is a serious limitation, particularly near dawn and dusk, where longitudinal drifts are expected to be large. Partly to extend tracking capabilities, direction-finding techniques have recently been developed that should permit measurement of both components of drift by tracking the motions of ionospheric exit points of whistler ducts in both the east-west and the north-south directions. A coordinated multinational program of broadband VLF recording and direction finding is scheduled to be carried out as a part of antarctic contributions to the International Magnetospheric Study during 1977–1979.

The successful transmitter operation at Siple suggests that transmitted signals with appropriate frequency modulation can provide a valuable complement to natural whistlers in the area of thermal plasma diagnostics. The travel time of transmitter signals measured as a function of frequency provides essentially the same information afforded by natural whistlers for the purpose of measuring thermal plasma parameters. Although a transmitter has obvious limitations in power and in duration of operation, it offers the important advantage of controlled sampling rates. Under favorable conditions, phase measurements of constant-frequency transmitter signals [*McNeil*, 1967; *Thomson*, 1975] can be combined with the conventional whistler technique to improve measurement precision greatly.

Wave amplification and emission generation in the magnetosphere are intimately connected with the energetic particle distribution. A major thrust in future VLF research should be aimed at understanding wave-particle interactions in sufficient quantitative detail to permit the use of wave amplitude information for energetic particle diagnostics. This will require further phenomenological studies of naturally occurring emissions and wave amplification as well as controlled wave-particle interaction experiments and theoretical modeling.

All ground-based observations of magnetospheric wave phenomena depend on the existence of ducts that guide the waves through the ionosphere. However, little is known of the details of the ducting process. Comparisons between ground and satellite data show that wave activity in the unducted mode has little resemblance to that in the ducted mode [e.g., *Smith and Angerami*, 1968]. On the other hand, there is clear evidence that significant amounts of wave energy leak out of ducts, thus contributing to unducted activity [e.g., *Angerami*, 1970]. It is important to learn how the total wave energy in the magnetosphere is divided between ducted and unducted modes and how the energy is transferred from one mode to the other.

It was pointed out earlier that particle precipitation from the magnetosphere is a major source of ionization in the nighttime lower ionosphere. The role of VLF waves, both natural and man-made, in *D* and *E* region dynamics must be evaluated quantitatively. This requires simultaneous observations of VLF waves and accompanying ionospheric perturbations by using HF sounders, X ray and optical emission detectors, riometers, etc.

*Acknowledgments*. This work was supported in part by the National Science Foundation, Division of Polar Programs, under grant DPP-74-04093 and in part by the National Science Foundation, Atmospheric Sciences Section, under grants ATM-74-20084 and ATM-75-07707.

## REFERENCES

Angerami, J. J., A whistler study of the distribution of thermal electrons in the magnetosphere, Ph.D. thesis, Elec. Eng. Dep., Stanford Univ., Stanford, Calif., 1966.

Angerami, J. J., Whistler duct properties deduced from VLF observation made with the Ogo 3 satellite near the magnetic equator, *J. Geophys. Res.*, *75*, 6115, 1970.

Angerami, J. J., and D. L. Carpenter, Whistler studies of the plasmapause in the magnetosphere, 2, Equatorial density and total tube electron content near the knee in magnetospheric ionization, *J. Geophys. Res.*, *71*, 711, 1966.

Axford, W. I., Magnetospheric convection, *Rev. Geophys. Space Phys.*, *7*, 421, 1969.

Banks, P. M., and T. E. Holzer, Features of plasma transport in the upper atmosphere, *J. Geophys. Res.*, *74*, 6304, 1969.

Banks, P. M., J. R. Doupnik, and S.-I. Akasofu, Electric field observations by incoherent scatter radar in the auroral zone, *J. Geophys. Res.*, *78*, 6607, 1973.

Barrington, R. E., T. R. Hartz, and R. W. Harvey, Diurnal distribution of ELF, VLF, and LF noise at high latitudes as observed by Alouette 2, *J. Geophys. Res.*, *76*, 5278, 1971.

Bell, T. F., ULF wave generation through particle precipitation induced by VLF transmitters, *J. Geophys. Res.*, *81*, 3316, 1976.

Block, L. P., Potential double layers in the ionosphere, *Cosmic Electrodynamics*, *3*, 349, 1972.

Block, L. P., and D. L. Carpenter, Derivation of magnetospheric electric fields from whistler data in a dynamic geomagnetic field, *J. Geophys. Res.*, *79*, 2783, 1974.

Brice, N., Bulk motion of the magnetosphere, *J. Geophys. Res.*, *72*, 5193, 1967.

Brice, N. M., and R. L. Smith, Recordings from satellite Alouette 1, a very-low-frequency plasma resonance, *Nature*, *203*(4948), 926, 1964.

Bullough, K., and J. L. Sagredo, VLF goniometer observations at Halley Bay, Antarctica, 1, The equipment and the measurement of signal bearing, *Planet. Space Sci.*, *21*, 899, 1973.

Burton, E. T., and E. M. Boardman, Audio-frequency atmospherics, *Proc. IRE, 21,* 1476, 1933.

Carpenter, D. L., The magnetosphere during magnetic storms: A whistler analysis, Ph.D. thesis, Elec. Eng. Dep., Stanford Univ., Stanford, Calif., 1962.

Carpenter, D. L., Whistler evidence of a 'knee' in the magnetospheric ionization density profile, *J. Geophys. Res., 68,* 1675, 1963.

Carpenter, D. L., Whistler studies of the plasmapause in the magnetosphere, 1, Temporal variations in the position of the knee and some evidence on plasma motions near the knee, *J. Geophys. Res., 71,* 693, 1966.

Carpenter, D. L., Ducted whistler mode propagation in the magnetosphere: A half-gyrofrequency upper intensity cutoff and some associated wave growth phenomena, *J. Geophys. Res., 73,* 2919, 1968.

Carpenter, D. L., Whistler evidence of the dynamic behavior of the duskside bulge in the plasmasphere, *J. Geophys. Res., 75,* 3837, 1970.

Carpenter, D. L., and C. G. Park, On what ionospheric workers should know about the plasmapause-plasmasphere, *Rev. Geophys. Space Phys., 11,* 133, 1973.

Carpenter, D. L., and N. Seely, Cross-$L$ plasma drifts in the outer plasmasphere: Quiet time patterns and some substorm effects, *J. Geophys. Res., 81,* 2728, 1976.

Carpenter, D. L., and K. Stone, Direct detection of a whistler method of the magnetospheric electric field associated with a polar substorm, *Planet. Space Sci., 15,* 395, 1967.

Carpenter, D. L., F. Walter, R. E. Barrington, and D. J. McEwen, Alouette 1 and 2 observations of abrupt changes in whistler rate and of VLF noise variations at the plasmapause: A satellite-ground study, *J. Geophys. Res., 73,* 2929, 1968.

Carpenter, D. L., K. Stone, and S. Lasch, A case study of artificial triggering of VLF magnetospheric noise during the drift of a whistler duct across magnetic shells, *J. Geophys. Res., 74,* 1848, 1969.

Carpenter, D. L., K. Stone, J. C. Siren, and T. L. Crystal, Magnetospheric electric fields deduced from drifting whistler paths, *J. Geophys. Res., 77,* 2819, 1972.

Cauffman, D. P., and D. A. Gurnett, Satellite measurements of high latitude convection electric fields, *Space Sci. Rev., 13,* 369, 1972.

Chappell, C. R., Detached plasma regions in the magnetosphere, *J. Geophys. Res., 79,* 1861, 1974.

Chappell, C. R., K. K. Harris, and G. W. Sharp, A study of the influence of magnetic activity on the location of the plasmapause as measured by Ogo 5, *J. Geophys. Res., 75,* 50, 1970.

Corcuff, P., and Y. Corcuff, Détermination des paramètres $f_n$, $t_n$ charactéristiques des sifflements radioélectriques reçus au sol, *Ann. Geophys., 29,* 273, 1973.

Corcuff, Y., La dispersion des sifflements radioélectriques au cours des orages magnétiques: Ses variations nocturne, annuelle et semi-annuelle en periodes calmes, *Ann. Geophys., 18,* 334, 1962.

DeWitt, R. N., and S.-I. Akasofu, Dynamo action in the ionosphere and motions of the magnetospheric plasma, 1, Symmetric dynamo action, *Planet. Space Sci., 12,* 1147, 1964.

Dunckel N., B. Ficklin, L. Rorden, and R. A. Helliwell, Low-frequency noise observed in the distant magnetosphere with Ogo 1, *J. Geophys. Res., 75,* 1854, 1970.

Edgar, B. C., The structure of the magnetosphere as deduced from magnetospherically reflected whistlers, Ph.D. thesis, Elec. Eng. Dep., Stanford Univ., Stanford, Calif., 1972.

Edgar, B. C., The upper and lower frequency cutoffs of magnetospherically reflected whistlers, *J. Geophys. Res., 81,* 205, 1976.

Evans, J. V., Measurements of horizontal drifts in the $E$ and $F$ regions at Millstone Hill, *J. Geophys. Res., 77,* 2341, 1972.

Geisler, J. E., On the limiting daytime flux of ionization into the protonosphere, *J. Geophys. Res., 72,* 81, 1967.

Grebowsky, J. M., N. C. Maynard, Y. K. Tulunay, and L. J. Lanzerotti, Coincident observations of ionospheric troughs and the equatorial plasmapause, *Planet. Space Sci., 25,* in press, 1977.

Gringauz, K. I., V. G. Kurt, V. I. Moroz, and I. S. Shklovskii, Results of observations of charged particles observed out to $R$ = 100,000 km, with the aid of charged-particle traps on Soviet space rockets, *Astron. Zh., 37,* 716, 1960.

Gurnett, D. A., A satellite study of VLF hiss, *J. Geophys. Res., 71,* 5599, 1966.

Gurnett, D. A., The earth as a radio source: Terrestrial kilometric radiation, *J. Geophys. Res., 79,* 4227, 1974.

Gurnett, D. A., and L. A. Frank, VLF hiss and related plasma observations in the polar magnetosphere, *J. Geophys. Res., 77,* 172, 1972.

Hanson, W. B., and I. B. Ortenburger, The coupling between the protonosphere and the normal $F$ region, *J. Geophys. Res., 66,* 1425, 1961.

Hanson, W. B., and T. N. L. Patterson, The maintenance of the nighttime $F$-layer, *Planet. Space Sci., 12,* 979, 1964.

Helliwell, R. A., Exospheric electron density variations deduced from whistlers, *Ann. Geophys., 17,* 76, 1961.

Helliwell, R. A., *Whistlers and Related Ionospheric Phenomena*, Stanford University Press, Stanford, Calif., 1965.

Helliwell, R. A., and J. P. Katsufrakis, VLF wave injection into the magnetosphere from Siple Station, Antarctica, *J. Geophys. Res., 79,* 2511, 1974.

Helliwell, R. A., J. H. Crary, J. H. Pope, and R. L. Smith, The 'nose' whistler: A new high-latitude phenomenon, *J. Geophys. Res., 61,* 139, 1956.

Helliwell, R. A., J. P. Katsufrakis, and M. L. Trimpi, Whistler-induced amplitude perturbation in VLF propagation, *J. Geophys. Res., 78,* 4679, 1973.

Helliwell, R. A., J. P. Katsufrakis, T. F. Bell, and R. Raghuram, VLF line radiation in the earth's magnetosphere and its association with power system radiation, *J. Geophys. Res., 80,* 4249, 1975.

Heppner, J. P., Electric field variations during substorms: Ogo-6 measurements, *Planet. Space Sci., 20,* 1475, 1972.

Ho, D., Interaction between whistlers and quasi-periodic VLF emissions, *J. Geophys. Res., 78,* 7347, 1973.

Ho, D., and L. C. Bernard, A fast method to determine the nose frequency and minimum group delay of a whistler when the causative spheric is unknown, *J. Atmos. Terr. Phys., 35,* 881, 1973.

Hoch, R. J., Stable auroral red arcs, *Rev. Geophys. Space Phys., 11,* 935, 1973.

James, H. G., VLF saucers, *J. Geophys. Res., 81,* 501, 1976.

Jørgensen, T. S., Interpretation of auroral hiss measured on Ogo 2 and at Byrd Station in terms of Cerenkov radiation, *J. Geophys. Res., 73,* 1055, 1968.

Kimura, I., Triggering of VLF magnetospheric noise by a low-power (100 W) transmitter, *J. Geophys. Res., 73,* 445, 1968.

Laaspere, T., and R. A. Hoffman, New results on the correlation between low-energy electrons and auroral hiss, *J. Geophys. Res., 81,* 524, 1976.

Lanzerotti, L. J., H. Fukunishi, and L. Chan, ULF pulsation evidence of the plasmapause, 3, Interpretation of polarization

and spectral amplitude studies of Pc 3 and Pc 4 pulsations near $L = 4$, *J. Geophys. Res., 79,* 4648, 1974.

Leavitt, M. K., A frequency-tracking direction finder for whistlers and other very low frequency signals, Ph.D. thesis, Elec. Eng. Dep., Stanford Univ., Stanford, Calif., 1975.

Lim, T. L., and T. Laaspere, An evaluation of the intensity of Cerenkov radiation from auroral electrons with energies down to 100 eV, *J. Geophys. Res., 77,* 4145, 1972.

Maeda, H., Electric fields in the magnetosphere associated with daily geomagnetic variations and their effect on trapped particles, *J. Atmos. Terr. Phys., 26,* 1133, 1964.

Maggs, J. E., Coherent generation of VLF hiss, *J. Geophys. Res., 81,* 1707, 1976.

Martyn, D. F., The morphology of the ionospheric variations associated with magnetic disturbances, 1, Variations at moderately low latitudes, *Proc. Roy. Soc., Ser. A, 218,* 1, 1953.

Matsushita, S., Interactions between the ionosphere and the magnetosphere for $S_q$ and $L$ variations, *Radio Sci., 6,* 279, 1971.

McNeil, F. A., Frequency shift on whistler mode signals from a stabilized VLF transmitter, *Radio Sci., 2,* 589, 1967.

Morozumi, H. M., and R. A. Helliwell, A correlation study of the diurnal variation of upper atmospheric phenomena in the southern auroral zone, *Tech. Rep. 2,* Radioscience Lab., Stanford Electron. Labs., Stanford Univ., Stanford, Calif., 1966.

Mozer, F. S., Magnetospheric dc electric field: Present knowledge and outstanding problems to be solved during the IMS, in *The Scientific Satellite Programme During the International Magnetospheric Study*, edited by K. Knott and B. Battrick, p. 101, D. Reidel, Hingham, Mass., 1976.

Muldrew, D. B., *F* layer ionization troughs deduced from Alouette data, *J. Geophys. Res., 70,* 2635, 1965.

Murphy, J. A., G. J. Bailey, and R. J. Moffett, Calculated variations in the $H^+$ content of the plasmasphere, *Geophys. J. Roy. Astron. Soc., 41,* 319, 1975.

Nishida, A., Formation of plasmapause, or magnetospheric plasma knee, by the combined action of magnetospheric convection and plasma escape from the tail, *J. Geophys. Res., 71,* 5669, 1966.

Oguti, T., Hiss-emitting auroral activity, *J. Atmos. Terr. Phys., 37,* 761, 1975.

Park, C. G., Whistler observations of the interchange of ionization between the ionosphere and the protonosphere, *J. Geophys. Res., 75,* 4249, 1970.

Park, C. G., Methods of determining electron concentration in the magnetosphere from nose whistlers, *Tech. Rep. 3454-1,* Radioscience Lab., Stanford Electron. Labs., Stanford Univ., Stanford, Calif., 1972.

Park, C. G., Whistler observations of the depletion of the plasmasphere during a magnetospheric substorm, *J. Geophys. Res., 78,* 672, 1973.

Park, C. G., Some features of plasma distribution in the plasmasphere deduced from antarctic whistlers, *J. Geophys. Res., 79,* 169, 1974.

Park, C. G., Whistler observations during a magnetospheric sudden impulse, *J. Geophys. Res., 80,* 4738, 1975.

Park, C. G., Substorm electric fields in the evening plasmasphere and their effects on the underlying *F* layer, *J. Geophys. Res., 81,* 2283, 1976*a*.

Park, C. G., The role of manmade VLF signals and noise in wave-particle interactions in the magnetosphere, in *Physics of Solar Planetary Environments, Proceedings of the International Symposium on Solar-Terrestrial Physics*, vol. 2, edited by D. J. Williams, p. 772, AGU, Washington, D. C., 1976*b*.

Park, C. G., and P. M. Banks, Influence of thermal plasma flow on the mid-latitude nighttime $F_2$ layer: Effects of electric fields and neutral winds inside the plasmasphere, *J. Geophys. Res., 79,* 4661, 1974.

Park, C. G., and P. M. Banks, Influence of thermal plasma flow on the daytime $F_2$ layer, *J. Geophys. Res., 80,* 2819, 1975.

Park, C. G., and D. L. Carpenter, Whistler evidence of large-scale irregularities in the plasmasphere, *J. Geophys. Res., 75,* 3825, 1970.

Park, C. G., and C.-I. Meng, Distortions of the nightside ionosphere during magnetospheric substorms, *J. Geophys. Res., 78,* 3828, 1973.

Potemra, T. A., and A. J. Zmuda, Precipitating energetic electrons as an ionization source in the mid-latitude nighttime *D* region, *J. Geophys. Res., 75,* 7161, 1970.

Rosenberg, T. J., R. A. Helliwell, and J. P. Katsufrakis, Electron precipitation associated with discrete very low frequency emissions, *J. Geophys. Res., 76,* 8445, 1971.

Sagredo, J. L., and K. Bullough, VLF goniometer studies at Halley Bay, Antarctica, 2, Magnetospheric structure deduced from whistler observations, *Planet. Space Sci., 21,* 913, 1973.

Schieldge, J. P., Quiet-time currents and electric fields produced by the ionospheric dynamo, Ph.D. thesis, Univ. of Calif., Los Angeles, 1974.

Siren, J. C., Dispersive auroral hiss, *Nature, 238,* 118, 1972.

Siren, J. C., Fast hisslers in substorms, *J. Geophys. Res., 80,* 93, 1975.

Smith, A. J., I. D. Smith, and K. Bullough, Methods of determining whistler nose-frequency and minimum group delay, *J. Atmos. Terr. Phys., 37,* 1179, 1974.

Smith, R. L., The use of nose whistlers in the study of the outer ionosphere, Ph.D. thesis, Elec. Eng. Dep., Stanford Univ., Stanford, Calif., 1960.

Smith, R. L., Propagation characteristics of whistlers trapped in field-aligned columns of enhanced ionization, *J. Geophys. Res., 66,* 3699, 1961*a*.

Smith, R. L., Properties of the outer ionosphere deduced from nose whistlers, *J. Geophys. Res., 66,* 3709, 1961*b*.

Smith, R. L., VLF observations of auroral beams as sources of a class of emissions, *Nature, 224,* 351, 1969.

Smith, R. L., and J. J. Angerami, Magnetospheric properties deduced from Ogo 1 observations of ducted and nonducted whistlers, *J. Geophys. Res., 73,* 1, 1968.

Stiles, G. S., and R. A. Helliwell, Frequency-time behavior of artificially stimulated VLF emissions, *J. Geophys. Res., 80,* 608, 1975.

Storey, L. R. O., An investigation of whistling atmospherics, *Phil. Trans. Roy. Soc. London, Ser. A, 246,* 113, 1953.

Stubbe, P., Theory of the nighttime *F*-layer, *J. Atmos. Terr. Phys., 30,* 243, 1968.

Tarcsai, G., Routine whistler analysis by means of accurate curve fitting, *J. Atmos. Terr. Phys., 37,* 1447, 1975.

Taylor, H. A., Jr., The light ion trough, *Planet. Space Sci., 20,* 1593, 1972.

Taylor, H. A., Jr., and W. J. Walsh, The light ion trough, the main trough, and the plasmapause, *J. Geophys. Res., 77,* 6716, 1972.

Taylor, H. A., Jr., H. C. Brinton, and C. R. Smith, Positive ion composition in the magnetosphere obtained from Ogo A satellite, *J. Geophys. Res., 70,* 5769, 1965.

Taylor, W. W. L., and S. D. Shawhan, A test of incoherent

Cerenkov radiation for VLF hiss and other magnetospheric emissions, *J. Geophys. Res.*, *79*, 105, 1974.

Thomson, N. R., Whistler-mode signals: Group delay by cross correlation, *Geophys. Res. Lett.*, *2*, 451, 1975.

Titheridge, J. E., The maintenance of the night ionosphere, *J. Atmos. Terr. Phys.*, *30*, 1857, 1968.

Tsuruda, K., and K. Hayashi, Direction finding technique for elliptically polarized VLF electromagnetic waves and its application to the low-latitude whistlers, *J. Atmos. Terr. Phys.*, *37*, 1193, 1975.

Ungstrup, I. M., and D. L. Carpenter, 'Hisslers': Quasi-periodic ($T \sim 2$ s) VLF noise forms at auroral latitudes, *J. Geophys. Res.*, *79*, 5196, 1974.

Williams, D. J., and L. R. Lyons, Proton ring current and its interaction with the plasmapause: Storm recovery phase, *J. Geophys. Res.*, *79*, 4195, 1974.

Yonezawa, T., Maintenance of ionization in the nighttime $F2$ region, *Space Res.*, *5*, 49, 1965.